



Silane: A new linker for chromophores in dye-sensitised solar cells

Katherine Szpakolski^a, Kay Latham^{a,*}, Colin Rix^a, Rozina A. Rani^b, Kouros Kalantar-zadeh^b

^aSchool of Applied Sciences, RMIT University, GPO Box 2476V, Melbourne, VIC 3001, Australia

^bSchool of Electrical Communications Engineering, RMIT University, GPO Box 2476V, Melbourne, VIC 3001, Australia

ARTICLE INFO

Article history:

Available online 4 August 2012

This paper is dedicated to the life and works of Professor Alfred Werner (1866–1919) on the 100th anniversary of his award of Nobel Prize in Chemistry, and in recognition of his major contributions to the field of Coordination Chemistry.

Keywords:

Ruthenium
Polypyridyl complexes
Silane linkage
DSSCs
TiO₂
WO₃

ABSTRACT

A series of ruthenium(II) polypyridyl complexes, with novel silane functionalisation, [Ru(*bipy*)₂(*bipy-sil*)](PF₆)₂ (**3**), [Ru(*bipy-sil*)₂Cl₂] (**6**), and [Ru(*bipy-sil*)₂(NCS)₂] (**7**) have been synthesised and tested as chromophores (dyes) in TiO₂ and WO₃ based dye-sensitised solar cells (DSSCs). The performance of the respective DSSCs were compared to analogous dyes with ionic carboxylate ([Ru(*bipy*)₂(*dc**bipy*)](PF₆)₂ (**1**), [Ru(*dc**bipy*)₂Cl₂] (**4**), [Ru(*dc**bipy*)₂(NCS)₂] (**5**) or phosphonate ([Ru(*bipy*)₂(*dpipy*)](PF₆)₂ (**2**)) linking groups. The covalent silane–metal oxide linkage offers much needed improvement to the operating conditions, and lifetime of DSSCs, in terms of pH range and choice of solvent. UV–Vis spectroscopy of the deep-red solutions showed that the *bis-bipy-sil* complexes absorbed more visible light than the *tris-bipy* complex, as indicated by the presence of two absorption bands and higher ϵ values. The UV–Vis spectrum of (**3**) contained a single broad absorption at 400–600 nm with: $\lambda_{\max} = 457$ nm; $\epsilon = 10520 \pm 440$ L mol⁻¹ cm⁻¹, whereas two intense broad absorption bands were observed for novel *bis-bipy-sil* complexes (**6**): 340–370 nm ($\lambda_{\max(1)} = 365$ nm, $\epsilon_{(1)} = 12716 \pm 180$ L mol⁻¹ cm⁻¹); and 440–540 nm ($\lambda_{\max(2)} = 485$ nm, $\epsilon_{(2)} = 11070 \pm 150$ L mol⁻¹ cm⁻¹), and (**7**): 340–400 nm ($\lambda_{\max} = 371$ nm, $\epsilon_{(1)} = 20690 \pm 485$ L mol⁻¹ cm⁻¹), and 460–530 nm ($\lambda_{\max} = 500$ nm and $\epsilon_{(2)} = 20750 \pm 487$ L mol⁻¹ cm⁻¹). The bands in (**7**) being significantly more defined.

A 10-fold improvement in the efficiency of the *bipy-sil* TiO₂-based DSSCs was observed from (**3**) to (**6**) to (**7**). This performance was lower than that of the commercial N3 dye, [Ru(*dc**bipy*)₂(NCS)₂] (**5**), but the current of (**7**) on WO₃, was comparable to that of the carboxylate system (**4**). There is considerable potential for further improvement by modification of the silyl linker, reducing the long non-conjugated propyl chain between the amide group and the silatrane (*bipy-sil*), to a short, conjugated link. During an extensive synthetic study, the most promising strategy was identified as direct linkage, the formation of a direct Si–C bond, using butyllithium with 4,4'-dibromo-2,2'-bipyridine and either trimethylsilane or 1-ethoxysilatrane, provided that the product can be captured and stabilised prior to binding to a metal oxide coated DSSC substrate.

© 2012 Elsevier Ltd. All rights reserved.

1. Introduction

Dye-sensitised solar cells (DSSCs) – so called ‘Gratzel’ cells (Fig. 1), have the potential to make a significant contribution to solar energy capture as they perform the photo-voltaic conversion of solar radiation to electricity. However, despite considerable research effort, their commercial implementation has been hampered by high cost and low conversion efficiency. Proof-of-principle cells have been developed in the laboratory, but are generally based on expensive metals, particularly ruthenium, and only have photo-voltaic conversions of the order of 10% [1,2].

Such cells are based on a redox-active chromophore, which can be an organic ‘dye’ or a transition metal co-ordination compound having a broad absorption range across the solar spectrum, usually

in the visible and ultra-violet region (Ru(II) complexes coordinated to N-heterocycles have been explored extensively due to their photochemical and photophysical behaviour) [3,4]. Following electronic excitation, the chromophore then needs to possess a sufficiently long-lived excited state (i.e. a fluorescent or phosphorescent state) which allows the excited electron to be passed to an external circuit, usually via a semi-conducting substrate such as titanium dioxide, or a variety of other metal oxides, incorporating metals such as Sn [5], Zn [6], W [7], and Nb [8]. This step is a major stumbling block in the efficient energy capture and conversion process, since although relatively efficient chromophores are available, it is the rate of electron transfer to the substrate that limits the photo-current. This step is not only dependent on the life-time of the excited electronic state, but also relies critically on efficient electron transfer from the molecular orbitals centred on the chromophore, to those in the conduction band of the substrate. It is therefore dependent on the proximity of the exchanging

* Corresponding author. Fax: +61 3 9925 3747.

E-mail address: kay.latham@rmit.edu.au (K. Latham).

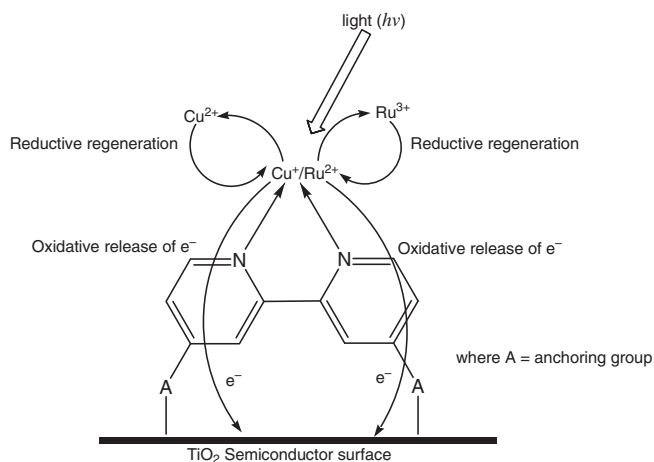


Fig. 1. Schematic of dye complex ($\text{Cu}^+/\text{Cu}^{2+}$ and $\text{Ru}^{2+}/\text{Ru}^{3+}$ systems), anchored to a semiconductor substrate in a DSSC (regenerative cell), absorbing light and transferring the excited electron to the semiconductor substrate.

centres, and the presence of an electron-conducting pathway between them. Hence, the nature of the attachment of the chromophore to the surface of the metal oxide is especially important.

The use of highly polar carboxylate (COO^-) and phosphonate ($\text{P}(\text{O})_2(\text{OH})^-$ or PO_3^{2-}) ionic linker groups, to anchor the appropriate metal-based chromophore to a metal-oxide surface, has been explored extensively in previous studies [4,9–24], but the surface binding of these groups to metal oxides is not stable over the full pH range, and they are not compatible with some organic solvents [15,25]. To overcome these deficiencies, a covalent linker was deemed necessary. The purpose of the current report is to explore a new linker, a silyl ester, which may, by skilful design, improve the efficiency of electron transfer between the chromophore and metal-oxide semiconductor substrate.

One of the many reasons why silyl coupling has not been explored is the rather tedious synthetic procedure required to prepare appropriate precursor ligands [26,27]. An *in-situ* synthetic method has been reported [26], whereby the first step involved modification of titania with organoalkoxysilane materials (3-chloropropyl-methoxysilane), but this investigation focused on photocatalytic activity for the degradation of phenols. It is, however, still representative of a silyl linkage to a metal oxide. A silyl linkage has also been prepared by *in-situ* pyrazole silylation on the ruthenium complex, $[\text{Ru}(\text{py-pzH})_3]^{2+}$ (where *py-pzH* = 3-(2'-pyridyl)pyrazole), Fig. 2 [28]. Although these linkers have not been exploited to any degree in DSSCs, Brennan et al. [29] have investigated silicon-oxygen based linkages with SnO_2 semiconducting surfaces, and found the silyl-ester bond a promising alternative linker to carboxylates and phosphonates. To this end, the potential for anchoring of 'dyes'

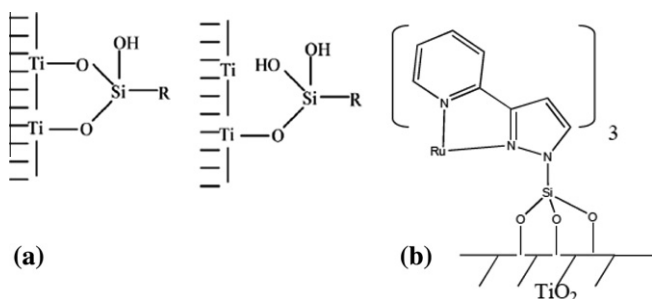


Fig. 2. Possible linkage of silyl to TiO_2 , where R = (a) a palladium 2-aminothiazole complex [20], and (b) $[\text{Ru}(\text{py-pzH})_3]^{2+}$ (where *py-pzH* = 3-(2'-pyridyl)pyrazole) [22].

to a range of metal oxides (e.g. TiO_2 , WO_3) using silyl groups is explored within this paper.

The synthesis of two novel *bis-bipyridyl* ruthenium(II) complexes which contain a silatrane-propyl amide link on the (4,4'-dicarboxylic acid)-2,2'-bipyridine ligand (*bipy-sil*) are reported, and their photophysical properties, and efficiency as dyes in TiO_2 and WO_3 - based DSSCs, tested and compared against carboxylic acid and phosphonate functionalised *bipy* analogues (*dcbipy* and *dpbipy* respectively) (Fig. 3). In addition, an extensive study, which concentrated on strategies to synthesise pyridine-type ligands with short distances between the silatrane linker and the pyridine ring, was undertaken.

2. Materials and methods

Unless otherwise stated, all chemicals were of at least analytical reagent grade and used without further purification. Ammonium hexafluorophosphate (95%), 2,2-bipyridine (*bipy*, 99%) *n*-butyllithium in hexane (1.567 M), and triethylphosphite (98%) from Aldrich Chemicals. Triisopropyl phosphite (90%) from Alfa Aesar. Triethanolamine ($\geq 98\%$), triethylamine ($\geq 99\%$), and triphenylphosphine, ($\geq 98\%$) from BDH Chemicals. 4,4'-Dibromo-2,2'-bipyridine and 4,4'-dicarboxylic acid-2,2'-bipyridine (*dcbipy*) from Carbosynth and Dyesol, respectively. Hexamethyldisilazane (*bis*(trimethylsilyl)amine, 98%) and thionyl chloride ($\geq 98\%$) from Merck. (3-aminopropyl)triethoxysilane ($\geq 98\%$), nicotinamide (98%), and tetraethylorthosilicate (99%) from Sigma Chemicals, and ruthenium(III) chloride hydrate (99.9%) and tetrakis(triphenylphosphine)palladium(0) (99.9%) from Strem Chemicals.

2.1. 1-(3'-Aminopropylsilatrane)

1-(3'-Aminopropylsilatrane) was synthesised following the procedure of Semenov [30]. A mixture of 3-aminopropyl(triethoxy)silane (8.84 g, 0.04 mol) and triethanolamine (5.69 g, 0.04 mol) was heated ($\sim 70^\circ\text{C}$) in a flask fitted with a Dean-Stark apparatus, and the ethanol produced was removed as it formed. The product was recrystallised twice, from toluene and then chloroform, to give a pale yellow powder in 62% yield. IR (KBr): $\nu = 3411$ (b), 2954 (m), 2900 (m), 1660(m), 1576 (m), 1494 (b), 1124 (m), 1096 (m), 946 (s), 917 (s), 778 (m) cm^{-1} . (where b = broad, m = medium and s = strong); ^1H NMR (CDCl_3 , 300 MHz): δ 0.4 (t, 2H, $J = 5$ Hz, $-\text{CH}_2-\text{Si}-$), 1.53 (m, 2H, $-\text{CH}_2-$), 2.60 (t, 6H, $J = 4.5$ Hz, $-\text{CH}_2-\text{N}$), 2.79 (t, 2H, $J = 3.5$ Hz, CH_2-NH_2), 3.75 (t, 6H, $J = 2.5$ Hz, $\text{CH}_2-\text{O}-$) ppm.

2.2. 1-Ethoxysilatrane

1-Ethoxysilatrane was prepared using a similar procedure to that described for 1-(3'-aminopropylsilatrane), however a large excess of benzene was added to act as an azeotropiser. A mixture of tetraethylorthosilicate (8.33 g, 0.04 mol), triethanolamine (5.69 g, 0.04 mol) and benzene (20 mL) were heated ($\sim 70^\circ\text{C}$) in a flask fitted with a Dean-Stark apparatus; the benzene-ethanol azeotrope produced was removed as formed. The product was recrystallised twice from toluene and then chloroform, to give a yellow solid in 73% yield. ^1H NMR (CDCl_3-d_6 , 300 MHz): δ 1.10 (t, 3H, $J = 6$ Hz, CH_3-), 2.6 (t, 6H, $J = 4$ Hz, CH_2-N), 3.9 (m, 2H, CH_2-O), 3.9 (m, 6H, $\text{O}-\text{CH}_2$) ppm.

2.3. 1-Chlorosilatrane

1-Chlorosilatrane was prepared following the procedure of Kazakova et al. [31] 1-ethoxysilatrane (220 mg, 1 mmol) was reacted with excess thionyl chloride (0.4 mL, 5 mmol) under a

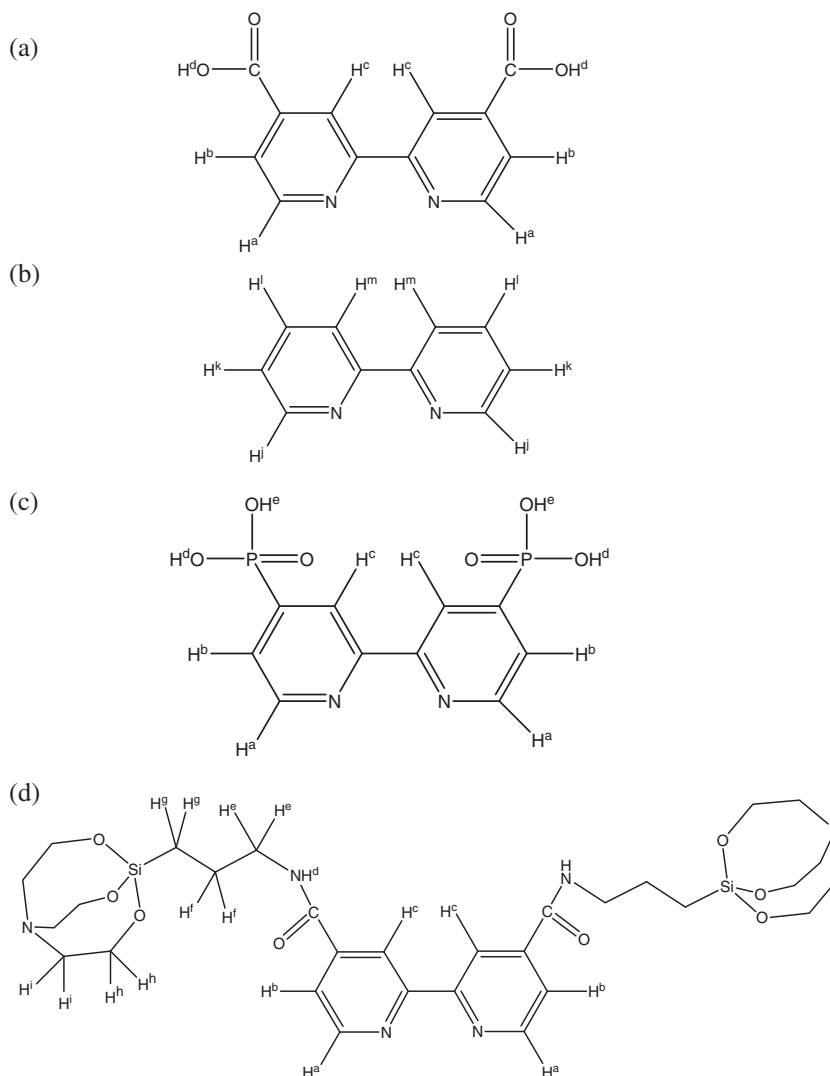


Fig. 3. Location of protons on (a) *dcbipy*, (b) *bipy*, (c) *dpbipy*, and (d) *bipy-sil* for ^1H NMR.

nitrogen atmosphere for 4 h. The excess thionyl chloride was removed under reduced pressure, and the product recrystallised from DCM and recovered as a white powder in 80% yield.

2.4. 2,2'-Bipyridine-4,4'-dicarboxylic acid bis[(3-silatranylpropyl) amide] (*bipy-sil*)

2,2'-Bipyridine-4,4'-dicarboxylic acid bis[(3-silatranylpropyl) amide] (*bipy-sil*) was synthesised following the procedure of Brennan et al. [29] 2,2'-bipyridine-4,4'-dicarboxylic acid (371 mg, 1.52 mmol) and thionyl chloride (4 mL, 55 mmol) were refluxed under nitrogen for 3 h, and any remaining unreacted thionyl chloride was removed under vacuum. To this, a solution containing triethylamine (450 μL , 3.23 mmol) and dichloromethane (5 mL, 78 mmol) was added. This mixture was then transferred to a solution of toluene (15 mL) containing 3-aminopropylsilatrane (712 mg, 3.06 mmol) and heated at 60 $^\circ\text{C}$ for 1 h, and then stirred at ambient temperature for 12 h. The solvent was removed under vacuum and the dark yellow product purified by column chromatography on silica gel (9 CHCl_3 : 1 CH_3OH) to give a white powder in 10% yield. IR (KBr): $\nu = 3456$ (b), 2937 (m), 2891 (m), 1659 (s), 1540 (s), 1463 (s), 1280 (s), 1119 (s), 1094 (s), 757 (s) cm^{-1} ; ^1H NMR (DMSO- d_6 , 300 MHz): δ 0.35 (t, 4H, $J = 6$ Hz, $-\text{CH}_2-\text{Si}-$), 1.50 (m,

4H, $-\text{CH}_2-$), 2.66 (t, 12H, $J = 5$ Hz, $-\text{CH}_2-\text{N}$), 2.84 (t, 4H, $J = 4$ Hz, CH_2-NH_2), 3.75 (t, 12H, $J = 4$ Hz, $\text{CH}_2-\text{O}-$), 7.8 (m, 2H, Ar-H), 8.05 (s, 2H, Ar-H), 8.6 (m, 2H, Ar-H) ppm.

2.5. 4,4'-Disilatrane-2,2'-bipyridine

2.5.1. Attempt (1) – Grignard method

In a 250 mL two-neck round bottom flask¹ fitted with a reflux condenser, a rubber septum and a stir bar, a mixture of 1-ethoxysilatrane (1.33 g, 6 mmol), anhydrous THF (10 mL), freshly washed magnesium turnings (121.5 mg, 5 mmol) and a small crystal of iodine² was heated to 70 $^\circ\text{C}$ under a nitrogen atmosphere. Then, a concentrated THF solution containing 4,4'-dibromo-2,2'-bipyridine (314 mg, 1 mmol) was added dropwise via syringe over half an hour. The mixture was allowed to reflux for an additional 3 h. The solvent was removed under reduced pressure, and hexane (30 mL) added to the crude product. The resulting mixture was filtered, and an off-white precipitate formed within a day. Spectroscopic examination (NMR, IR) of the white precipitate indicated that starting material was isolated.

¹ Glassware was flame dried before use.

² The same method was used with dibromoethane (375 mg, 2 mmol).

2.5.2. Attempt (2) – palladium method

Anhydrous toluene (33 mL) containing 4,4'-dibromo-2,2'-bipyridine (500 mg, 1.6 mmol), 1-ethoxysilatrane (1.5 g, 7 mmol), triethylamine (1.0 mL, 7 mmol), triphenylphosphine (2.1 g, 8 mmol) and Pd(PPh₃)₄ (0.37 g, 0.32 mmol) were refluxed for 18 h under nitrogen. The solution was filtered and distilled. A milky-white liquid product was isolated. Spectroscopic examination (NMR) of the milky-white liquid indicated that starting material was isolated.

2.5.3. Attempt (3) – butyllithium method

An attempt was made to synthesise 4,4'-disilatrane-2,2'-bipyridine following the procedure of Reidmiller et al. [32], with some modification. In a 100 mL two-neck round bottom flask¹ fitted with two rubber septums and a stir bar under a nitrogen atmosphere, a solution of 4,4'-dibromo-2,2'-bipyridine (100 mg, 0.32 mmol) in anhydrous diethyl ether (5 mL), a solution of *n*-butyllithium in hexane (0.2 mL, 1.567 M, 0.32 mmol) was added dropwise whilst cooling to –78 °C. The resulting solution was stirred and maintained at –78 °C for 1 h. A pre-cooled (–78 °C) solution of 1-ethoxysilatrane (140 mg, 0.64 mmol) in anhydrous diethyl ether (5 mL) was added to the former solution slowly via cannula. The resulting solution was stirred and maintained at –78 °C for 1 h, after which the solution was allowed to warm to room temperature. The solvent was evaporated and pentane (5 mL) added to the residue. The solution was filtered and the product isolated by distillation. A yellow liquid product was isolated. Spectroscopic examination (NMR) of the yellow liquid indicated the presence of aromatic and silatrane peaks, although not in correct ratios. The product decomposed rapidly, preventing further analysis by other methods.

2.5.4. Attempt (3a) – butyllithium and 1-chlorosilatrane

An attempt was made to synthesise 4,4'-disilatrane-2,2'-bipyridine following the procedure of Anderson et al. [33], with some modification. In a 100 mL two-neck round bottom flask, fitted with two rubber septums and a stir bar, and under a nitrogen atmosphere, a solution of *n*-butyllithium in hexane (0.2 mL, 1.567 M, 0.32 mmol) was added dropwise to a solution of 4,4'-dibromo-2,2'-bipyridine (100 mg, 0.32 mmol) in anhydrous diethyl ether (5 mL), whilst cooling to –78 °C. The resulting solution was stirred and maintained at –78 °C for 1 h. A pre-cooled (–78 °C) solution of 1-chlorosilatrane (133 mg, 0.64 mmol) in anhydrous diethyl ether (15 mL) was added to the former solution slowly via cannula. The resulting solution was stirred and maintained at –78 °C for 1 h, after which the solution was allowed to warm to room temperature. The solution was filtered and the product isolated by distillation. A yellow-brown liquid product was isolated. Spectroscopic examination (NMR) of the liquid indicated that only the starting materials had been recovered.

2.6. *N*-(Trimethylsilyl)pyridine-3-carboxamide

N-(Trimethylsilyl)pyridine-3-carboxamide was prepared following the procedure of Gilg et al. [34,35] A mixture of model compound, nicotinamide (250 mg, 2 mmol), chlorotrimethylsilane (224 mg, 2 mmol), and hexamethyldisilazane (2 mL) were refluxed for 5 h. A pale yellow powder was isolated in 65% yield. ¹H NMR (DMSO-*d*₆, 300 MHz): –0.1 (s, 3H, *J* = 6 Hz, CH₃-Si), 0.1 (s, 3H, CH₃-Si), 0.3 (s, 3H, CH₃-Si), 7.23 (m, 1H, Ar-H), 8 (m, 1H, Ar-H), 8.6 (dd, 1H, *J* = 5 Hz, 4.5 Hz, Ar-H), 8.9 (d, 1H, *J* = 3 Hz, Ar-H) ppm.

2.7. *N*-(1-Silatranyl)nicotinamide – attempted synthesis

An attempt was made to synthesise *N*-(1-silatranyl)nicotinamide following the procedure of Gilg et al. [34,35] with some modification. A mixture of nicotinamide (125 mg, 2 mmol), 1-chlo-

rosilatrane (214 mg, 1 mmol), and hexamethyldisilazane³ (2 mL) were refluxed for 5 h. A brown powder was isolated, which on spectroscopic examination (NMR) was identified as starting material was isolated.

2.8. 4,4'-Di(trimethylsilyl)-2,2'-bipyridine

4,4'-Di(trimethylsilyl)-2,2'-bipyridine was synthesised following the procedure of Anderson et al. [33], with some modification. In a 100 mL two-neck round bottom flask fitted with two rubber septums and a stir bar under a nitrogen atmosphere, a solution of *n*-butyllithium in hexane (0.2 mL, 1.567 M, 0.32 mmol) was added dropwise to a solution of 4,4'-dibromo-2,2'-bipyridine (100 mg, 0.32 mmol) in anhydrous diethyl ether (5 mL), whilst cooling to –78 °C. The resulting solution was stirred and maintained at –78 °C for 1 h. A pre-cooled (–78 °C) solution of TMS-Cl (70 mg, 0.64 mmol) in anhydrous diethyl ether (15 mL) was added to the former solution slowly via cannula. The resulting solution was stirred and maintained at –78 °C for 1 h, after which the solution was allowed to warm to room temperature. The solution was filtered and the product isolated by distillation. A yellow-brown liquid product was isolated. Spectroscopic examination (NMR) of the liquid indicated that 4,4'-di(trimethylsilyl)-2,2'-bipyridine was isolated in 12% yield. ¹H NMR (DMSO-*d*₆, 300 MHz): 0.4 (s, 9H, CH₃-Si), 7.2 (d, 1H, *J* = 3.5 Hz, Ar-H), 7.6 (d, 1H, *J* = 3 Hz, Ar-H), 8.5 (m, 2H, Ar-H), 8.7 (s, 2H, Ar-H) ppm.

2.9. 4,4'-Dicarboxysilylestere-silatrane-2,2'-bipyridine – attempted ester linkage

4,4'-Dicarboxysilylestere-silatrane-2,2'-bipyridine – attempted ester linkage following the procedure of Chen et al. [36], with some modification. In a two neck round bottom flask fitted with a Dean–Stark *dcbipy* (100 mg, 0.4 mmol), 1-ethoxysilatrane (90 mg, 0.4 mmol) and chlorobenzene (5 mL) were refluxed for 3 h under nitrogen. The ethanol and chlorobenzene were removed by azeotropic distillation. The pale yellow precipitate that formed was recrystallised from a 1:1 DCM/hexane solution. However, spectroscopic examination (NMR, IR) indicated that only starting material was isolated.

2.10. 2,2'-Bipyridine-4,4'-(diethyl phosphonate) (*depbipy*)

2,2'-Bipyridine-4,4'-(diethyl phosphonate) (*depbipy*) was synthesised following the procedure of Kanaizuka [37]. The product was purified by column chromatography on silica gel (99 CH₂Cl₂/1 CH₃-OH), to give a white powder in 76% yield. IR (KBr): ν = 3455 (b), 2149 (m), 1968 (m), 1637 (s), 1435 (s), 1398 (s), 1365 (s), 1227 (m), 1043 (m), 567 (m) cm⁻¹; ¹H NMR (CDCl₃, 300 MHz): δ 1.37 (t, 12H, *J* = 6 Hz, –CH₃), 4.20 (m, 8H, –CH₂–), 7.28 (s, 2H, Ar-H), 7.73 (dd, 2H, *J* = 4 Hz, 4.5 Hz, Ar-H), 8.82 (m, 2H, Ar-H) ppm.

2.11. Synthesis of complexes of Ru(II) with *bipy*, and ligands based on *bipy*

2.11.1. *cis*-[Ru(*bipy*)₂Cl₂]

cis-[Ru(*bipy*)₂Cl₂] was synthesised following the procedure of Sprintschnik et al. [38] A dark red-purple microcrystalline product was isolated in 65–70% yield. IR (KBr): ν = 3460 (b), 1602 (s), 1465 (s), 1445 (s), 1441 (s), 1315 (s), 1268 (s), 1159 (s), 1019 (s), 769 (s) cm⁻¹; ¹H NMR (D₂O/DMSO-*d*₆, 300 MHz): δ 7.47 (d, 4H, *J* = 4 Hz, Ar-H), 7.99 (m, 8H, Ar-H), 8.40 (d, 4H, *J* = 3.5 Hz, Ar-H) ppm.

³ The same method was used with toluene, benzene and chlorobenzene with similar results.

2.11.2. $[Ru(bipy)_2(dcbipy)](PF_6)_2$ (**1**)

Two synthetic methods were investigated for the synthesis of $[Ru(bipy)_2(dcbipy)](PF_6)_2$. The first synthesis followed the procedure of Browne et al. [39]. A red microcrystalline product was isolated in 58% yield. The second, and higher yielding $[Ru(bipy)_2(-dcbipy)](PF_6)_2$ synthesis, followed the procedure of Terpetschnig et al. [40]. A red microcrystalline product was isolated in 71% yield. IR(KBr): $\nu = 3463$ (b), 2936 (m), 1739 (s), 1608 (m), 1470 (s), 1449 (s), 1236 (m), 850 (s), 764 (s), 559 (s) cm^{-1} . 1H NMR (D_2O /DMSO- d_6 , 300 MHz): δ 7.20 (q, $J = 5$ Hz, Ar-H), 7.55 (dd, $J = 2$ Hz, 5 Hz, Ar-H), 7.60 (d, 4H, $J = 5$ Hz, Ar-H^m), 7.65 (d, 2H, $J = 5$ Hz, Ar-H^b), 7.82 (d, 2H, $J = 7$ Hz, Ar-H^a), 7.90 (m, 4H, Ar-H^k), 8.37 (d, 4H, Ar-H^j), 8.82 (s, 2H, Ar-H^c), 10.6 (s, 2H, -OH^d) ppm (see Fig. 3a and b for proton assignments).

2.11.3. $[Ru(bipy)_2(dpbipy)](PF_6)_2$ (**2**)

$[Ru(bipy)_2(dpbipy)](PF_6)_2$ (**2**) was prepared using the Terpetschnig et al. [40] procedure for $[Ru(bipy)_2(dcbipy)](PF_6)_2$, except *depbipy* (190 mg, 0.6 mmol) was used in place of *dcbipy*, and NaHCO₃ was not added. The diethyl ester was hydrolysed by adjusting the pH to 4 with HCl (4 M). A red microcrystalline product was isolated in 40% yield. IR(KBr): $\nu = 3484$ (b), 2993 (m), 1891 (s), 1589 (s), 1541 (s), 1485 (s), 1439 (s), 1191 (s), 1121 (s), 1027 (s), 723 (s), 698 (s) 538 (s) cm^{-1} . 1H NMR (D_2O /DMSO- d_6 , 300 MHz): δ 7.45–7.52 (m, Ar-H^{j,l,m}), 7.53–7.60 (m, Ar-H^{i,l,m}), 7.65–7.75 (m, Ar-H^{j,l,m}), 7.76 (dd, 2H, $J = 2$ Hz, 6 Hz, Ar-H^b), 8.54 (s, 2H, Ar-H^c), 8.79 (dd, 2H, $J = 1.5$ Hz, 9 Hz, Ar-H^a), 8.85 (t, $J = 6$ Hz, Ar-H^k) ppm. ^{31}P NMR (D_2O /DMSO- d_6 , 121.45 MHz): δ -10 (s, 2P, -P-) ppm (see Fig. 3b and c for proton assignments).

2.11.4. $[Ru(bipy)_2(bipy-sil)](PF_6)_2$ (**3**)

$[Ru(bipy)_2(bipy-sil)](PF_6)_2$ (**3**) was synthesised following the procedure of Brennan et al. [29]. $[Ru(bipy)_2Cl_2]$ (32 mg, 0.06 mmol) and *bipy-sil* (48 mg, 0.07 mmol) dissolved in DMF (3 mL) were heated to 90 °C under N₂ in subdued light for 72 h. Most of the solvent was then removed under vacuum and water (2 mL) added. The resulting solution was filtered, and to the filtrate was added a saturated NH₄PF₆ solution (0.4 mL). The solution was then extracted with ethyl acetate and the solvent recovered by distillation. A red powder was isolated in 42% yield. IR(KBr): $\nu = 3367$ (b), 2961 (m), 2896 (m), 1663 (s), 1551 (s), 1462 (s), 1277 (s), 1066 (m), 918 (s), 802 (s) cm^{-1} . 1H NMR (CDCl₃, 300 MHz): δ 0.30 (m, 4H, -CH₂^g-Si), 1.35 (m, 4H, -CH₂^f), 2.45 (t, 12H, $J = 6$ Hz, -CH₂ⁱ-N), 2.75 (m, 4H, -CH₂^e-NH), 3.29–3.70 (m, 12H, -CH₂^h-O), 7.27 (d, 4H, $J = 3$ Hz, Ar-H^m), 7.41 (d, 4H, $J = 2$ Hz, Ar-H^l), 7.45 (d, 2H, $J = 2.5$ Hz, Ar-H^b), 8.15 (d, 2H, $J = 2$ Hz, Ar-H^a), 8.20 (t, 4H, $J = 2$ Hz, Ar-H^k), 8.77 (m, 4H, Ar-H^j), 9.05 (s, 2H, Ar-H^c) ppm (see Fig. 3b and d for proton assignments). Elemental analysis calcd. (%) for C₅₀H₆₀N₁₀O₈Si₂RuP₂F₁₂ ($M_r = 1376.249$): C 43.64, H 4.39, N 10.18, P 4.50. Found (%): C 43.21, H 4.73, N 9.64, P 4.11.

2.11.5. *cis*- $[Ru(dcbipy)_2Cl_2]$ (**4**)

cis- $[Ru(dcbipy)_2Cl_2]$ (**4**) was synthesised following the procedure of Liska et al. [21]. RuCl₃·xH₂O (60 mg, 0.229 mmol) and *dcbipy* (113 mg, 0.463 mmol) were refluxed in DMF under N₂ for 8 h. The resulting solution was cooled slowly overnight, and then filtered. The majority of the DMF solvent was evaporated off to leave approximately 1 mL of solution. Acetone was then added dropwise until a dark-red precipitate formed. The precipitate was collected by filtration and dried under vacuum to give a 55% yield. IR(KBr): $\nu = 3467$ (b), 3115 (m), 2475 (b), 1989 (m), 1725 (s), 1660 (m), 1463 (s), 1368 (s), 1309 (s), 1142 (s), 1070 (s), 1014 (s), 767 (s), 685 (s) cm^{-1} . 1H NMR (D_2O , 300 MHz): δ 7.93 (d, 4H, $J = 4$ Hz, Ar-H^b), 8.84 (s, 4H, Ar-H^c), 8.91 (d, 4H, $J = 5$ Hz, Ar-H^a) ppm (see Fig. 3a for proton assignments). Note: In D_2O , proton exchange

can occur with -COOH^d to form -COOD and therefore the H^d proton would not be observed.

2.11.6. *cis*- $[Ru(dcbipy)_2(NCS)_2]$ 'N3 dye' (**5**)

cis- $[Ru(dcbipy)_2(NCS)_2]$ 'N3 dye' (**5**) was synthesised following the procedure of Nazeeruddin et al. [23]. The product was isolated as a dark red-microcrystalline powder 60% yield. IR(KBr): $\nu = 3449$ (b), 2929 (b), 2119 (s), 2002 (s), 1722 (s), 1637 (m), 1553 (s), 1407 (s), 1379 (s), 1308 (s), 1324 (s), 1025 (s), 771 (s) cm^{-1} ; 1H NMR (D_2O , 300 MHz): δ 7.97 (d, 4H, $J = 5$ Hz, Ar-H), 8.82 (s, 4H, Ar-H), 8.91 (d, 4H, $J = 5$ Hz, Ar-H) ppm (see Fig. 3a for proton assignments).

2.11.7. *cis*- $[Ru(bipy-sil)_2Cl_2]$ (**6**)

cis- $[Ru(bipy-sil)_2Cl_2]$ (**6**) was prepared using a similar procedure as *cis*- $[Ru(dcbipy)_2Cl_2]$ (**4**), except *bipy-sil* (100 mg, 0.1 mmol) was used in place of *dcbipy*. A dark red microcrystalline product was isolated in 40% yield. IR(KBr): $\nu = 3423$ (b), 2939 (m), 2892 (m), 1651 (s), 1551 (m), 1463 (s), 1281 (s), 1088 (s), 1022 (s), 916 (s), 759 (s) cm^{-1} . 1H NMR (DMSO- d_6 , 300 MHz): δ 0.40 (m, 4H, -CH₂^g-Si), 1.54 (m, 4H, -CH₂^f), 2.60 (m, 12H, -CH₂ⁱ-N), 2.81 (t, 4H, $J = 6$ Hz, -CH₂^e-NH), 3.70 (dt, 12H, $J = 6$ Hz, -CH₂^h-O), 7.75 (m, 4H, Ar-H^b), 8.76 (m, 4H, Ar-H^a), 8.78 (s, 2H, Ar-H^c) ppm (see Fig. 3d for proton assignments). Elemental analysis calcd. (%) for C₆₀H₈₈N₁₂O₁₆Si₄RuCl₂ ($M_r = 1517.740$): C 47.48, H 5.84, N 11.07, Cl 4.67. Found (%): C 47.88, H 5.36, N 11.32, Cl 4.20.

2.11.8. *cis*- $[Ru(bipy-sil)_2(NCS)_2]$ (**7**)

cis- $[Ru(bipy-sil)_2(NCS)_2]$ (**7**) was prepared from $[Ru(bipy-sil)_2Cl_2]$ (**6**). $[Ru(bipy-sil)_2Cl_2]$ (60 mg, 0.04 mmol) was dissolved in DMF (5 mL) under subdued light. In a separate beaker sodium thiocyanate (32 mg, 0.40 mmol) was dissolved in water (1 mL), and then added to the DMF solution. The resulting mixture was refluxed and stirred for 6 h under N₂. The solution was cooled slowly overnight, and the solvent removed under vacuum. The powder was dissolved in water and the suspension filtered through a sintered glass crucible. The solution was cooled to 4 °C for 18 h. The solution was allowed to warm to room temperature and within several hours a microcrystalline solid formed. This was filtered and subsequently washed with water, acetone and anhydrous diethyl ether. A dark red microcrystalline product was isolated in 35% yield. IR(KBr): $\nu = 3419$ (b), 3084 (b), 2945 (b), 2070 (s), 2000 (s), 1950 (s), 1664 (s), 1555 (s), 1470 (s), 1407 (s), 1104 (b) cm^{-1} ; 1H NMR (DMSO- d_6 , 300 MHz): δ 0.39 (m, 4H, -CH₂-Si), 1.55 (m, 4H, -CH₂-), 2.62 (m, 12H, -CH₂-N), 2.80 (t, 4H, $J = 5.5$ Hz, -CH₂-NH), 3.68 (m, 12H, -CH₂-O), 7.78 (m, 4H, Ar-H), 8.76 (m, 4H, Ar-H), 8.82 (s, 2H, Ar-H) ppm (see Fig. 3d for proton assignments). Elemental analysis calcd. (%) for C₆₂H₈₈N₁₄O₁₆S₂Si₄Ru ($M_r = 1563.001$): C 47.64, H 5.67, N 12.55, S 4.10. Found (%): C 47.72, H 5.34, N 12.25, S 4.45.

2.12. Preparation of semiconductors (TiO₂ and WO₃)

The TiO₂ substrates were purchased from Dyesol: they consist of a glass substrate with a TiO₂ coated area of 0.8 cm². The WO₃ substrates were prepared by the School of Electrical and Computer Engineering at RMIT University [7]. The dimensions of the glass substrates were 190 mm × 140 mm × 20 mm, and had a WO₃ coated area of 0.25 cm². The glass platelets of TiO₂/WO₃ substrates were annealed, prior to coating with 'dye', by placing them in a tube furnace open to the air. The substrates were then heated slowly (2 °C/min) from room temperature to 450 °C, and held at 450 °C for an hour and then cooled at a rate of 2 °C/min.

2.13. Preparation of test batch solar cells (TiO₂ and WO₃)

Dyes containing ruthenium complexes prepared in-house and possessing carboxylic or phosphonic linkages were coated on to the annealed semiconductor substrate by immersion in a 0.3 mM (acetonitrile or ethanol) solution of the dye, for 24 h. Dyes containing a silyl linkage were adhered to the semiconductor by immersing the oxide substrate in a 0.3 mM DMF solution of the dye and heating (~70 °C) for 1 h, in subdued light. In both cases a thin coloured film formed on the semiconductor, which was subsequently washed with ethanol and air dried. Two holes were then drilled into a second FTO-glass plate (FTO – fluorine doped tin oxide), the counter electrode; this was done to allow the injection of the liquid electrolyte. A heat-activated gasket (Surlyn[®]-30), with a film thickness of 30 μm was then placed around the dye-coated surface. The second FTO-glass plate was then placed on top and heated to approximately 100 °C. The liquid electrolyte, I⁻/I₃⁻ was then injected into the cell through the pre-drilled holes, approximately 1 drop in each hole. The holes were then sealed with a heat activated gasket. See Fig. 4 for solar cell schematic.

2.14. Solar cell testing unit

All cells containing the metal complex 'dye' were tested on a custom-made solar cell testing station [7]. The station comprised an ABET Technologies LS-120 solar light source fitted with an AM 1.5 filter, where the illumination power density was calibrated to 90 mW/cm², according to the protocol described by Zheng et al. [7]. Voltage and current measurements were collected using a Keithly 2602 sourcemeater.

2.15. Instrumental measurements

FT-IR absorption spectra were obtained on a Perkin Elmer Spectrum 100 spectrometer using KBr discs. The discs were prepared by grinding the sample (1–2 mg) and IR grade KBr (100 mg), into a homogeneous powder using a mortar and pestle. The powder was then placed in a die press (Specac 13 mm) and compacted under vacuum for approximately 5 min using 8 tonne of pressure. The spectra were collected using the following conditions: scan range 4000–400 cm⁻¹; number of scans 8; single beam; resolution: 4 cm⁻¹. Selected elemental analysis (C, H, N, S, P, halogens) was performed by the Campbell Microanalytical Laboratory at the University of Otago, New Zealand. NMR Spectra were collected using a Bruker AVANCE 300 MHz NMR spectrometer, at a frequency of 300 MHz for ¹H, 75.45 MHz for ¹³C and 121.45 MHz for ³¹P. Each sample was locked and shimmed for spectral optimisation. Samples were prepared using deuterated solvents: typically 20 mg of sample was dissolved in the appropriate solvent (either D₂O, CDCl₃ or DMSO-*d*⁶ (CD₃)₂SO) and placed in a 5 mm diameter glass NMR tube. UV-Vis spectra were then recorded on a Varian Cary 50 spectrophotometer, over the wavelength range 200–800 nm, at a scan

rate of 60 nm/min, and using a 1 cm path-length quartz UV cell. 50–100 mg of sample was dissolved in 25 mL of an appropriate solvent (water, ethanol, DMF, or acetonitrile). The molar extinction coefficient of the molecule (ϵ) can be calculated from the spectra using the Beer–Lambert Law:

$$A = \epsilon \times c \times l \quad (1)$$

(A = absorbance, c = concentration, l = path length).

3. Results and discussion

3.1. Preparation and characterisation of complexes

A series of ruthenium(II) coordination complexes containing either *bis*- or *tris*-*bipy* ligands were investigated (Table 1). Whilst the *tris*-chelated ruthenium complexes are known to be less efficient in terms of solar energy capture, not all of the ligands with anchoring groups could be incorporated into *bis*-chelated ruthenium complexes. For example, the *dpbipy* analogue could not be successfully prepared in a *bis*-form. Therefore, the *tris* complexes were used to compare the efficiency of various anchoring ligands and to make a reasonable comparison between existing ruthenium dyes and those prepared in this study.

The *bis*-*bipy* ruthenium dye complexes were synthesised by refluxing ruthenium(III) chloride with various 2,2'-bipyridine derivatives in DMF, under N₂, to form the ruthenium(II) *cis*-dichloro species (**4**, **6**) [21]. These were then refluxed with excess NaNCS to form the *cis*-dithiocyanato species (**5**, **7**) (Scheme 1). The N-coordinated thiocyanato group enabling fine-tuning of the physico-chemical properties of such ruthenium species, to optimise their function in a DSSC. The *tris*-*bipy* ruthenium complexes (**1**–**3**), whereby one of the *bipy* ligands contained a linker and the others were unsubstituted, were synthesised by refluxing [Ru(*bipy*)₂Cl₂] with various 2,2'-bipyridine derivatives in DMF under N₂. Each complex was precipitated from solution by addition of excess NH₄PF₆ (Scheme 2).

The reaction scheme for the preparation of the hydrolysis-resistant *bipy-sil* ligand is illustrated in Scheme 3. The *tris*-*bipy* ruthenium complex prepared by Brennan et al. [29], *bis*(2,2'-bipyridine)-4,4-dicarboxyl-(3-silatranylpropylamide)ruthenium(II) dihexafluorophosphate, [Ru(*bipy*)₂(*bipy-sil*)](PF₆)₂, was also prepared here, and numbered (**3**), together with two new *bis*-*bipy-sil* ruthenium complexes: [Ru(*bipy-sil*)₂Cl₂] (**6**), and [Ru(*bipy-sil*)₂(NCS)₂] (**7**). [Ru(*bipy-sil*)₂Cl₂] (**6**) was prepared by coordination of the *bipy-sil* ligand to ruthenium(III) trichloride, utilising methods published previously, but replacing *dcbipy* with *bipy-sil* (see Section 2). [Ru(*bipy-sil*)₂(NCS)₂] (**7**), was prepared by reacting [Ru(*bipy-sil*)₂Cl₂] (**6**) with excess sodium thiocyanate. All ligands and complexes were characterised using FT-IR, ¹H, ¹³C and, where possible, ³¹P NMR, UV-Vis spectroscopic analysis (see Section 2 for summary FTIR and NMR data; and Supplementary data for extended interpretation).

Table 1

Observed wavelength maxima (λ_{\max}) and molar extinction coefficient (ϵ) data for complexes (**1**)–(**7**).

Dye ^a	Number	λ_{\max} (nm)	ϵ (L mol ⁻¹ cm ⁻¹)
[Ru(<i>bipy</i>) ₂ (<i>dcbipy</i>)](PF ₆) ₂	(1)	460	14350
[Ru(<i>bipy</i>) ₂ (<i>dpbipy</i>)](PF ₆) ₂	(2)	450	17600
[Ru(<i>bipy</i>) ₂ (<i>bipy-sil</i>)](PF ₆) ₂	(3)	457	10520
[Ru(<i>dcbipy</i>) ₂ Cl ₂]	(4)	467	20790
[Ru(<i>dcbipy</i>) ₂ (NCS) ₂] N3	(5)	492	29630
[Ru(<i>bipy-sil</i>) ₂ Cl ₂]	(6)	485	11070
[Ru(<i>bipy-sil</i>) ₂ (NCS) ₂]	(7)	500	20750

^a The *dcbipy*, *dpbipy* and *bipy-sil* ligands in complexes (**1**)–(**7**) are shown in Scheme 1.

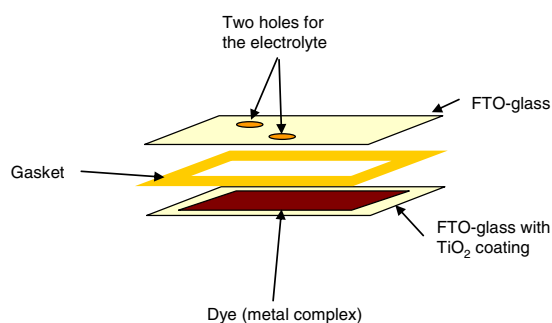
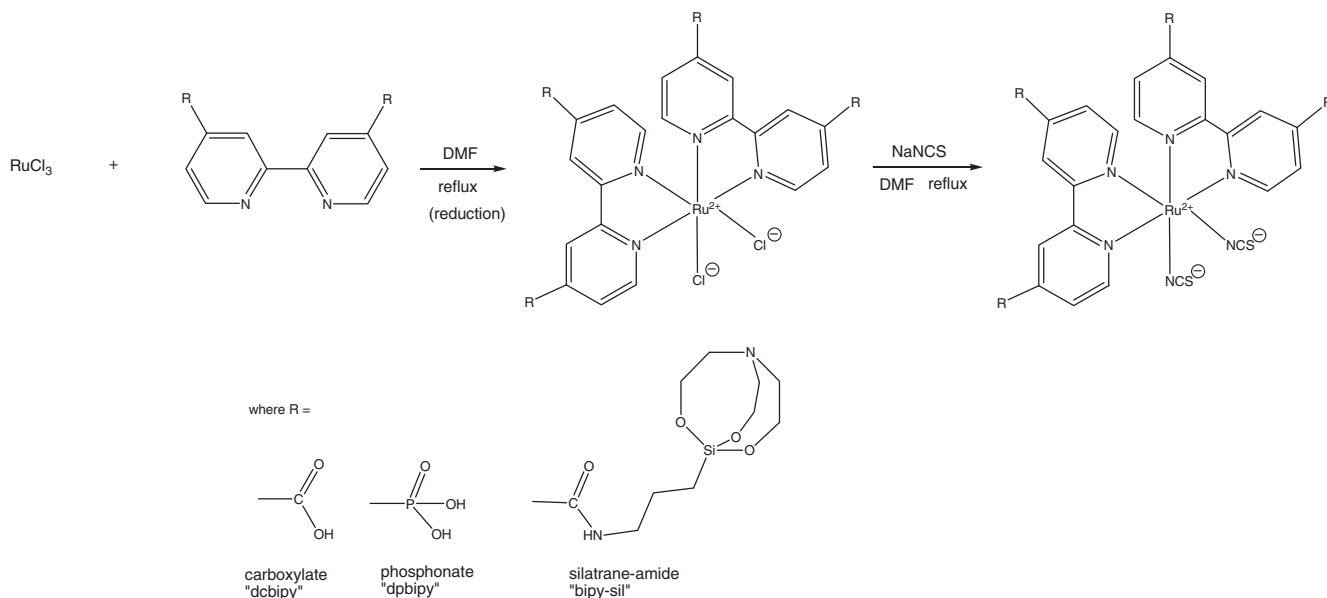
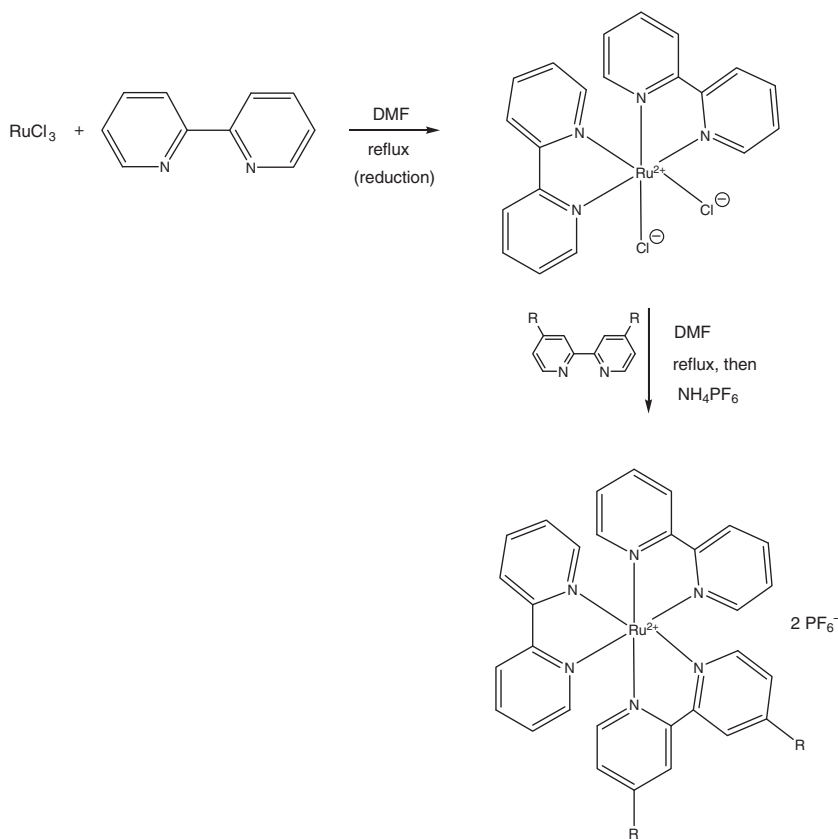


Fig. 4. Schematic of DSSC.



Scheme 1. Overall reaction sequence for the formation of bis-chelated Ru(II) complexes (4–7).



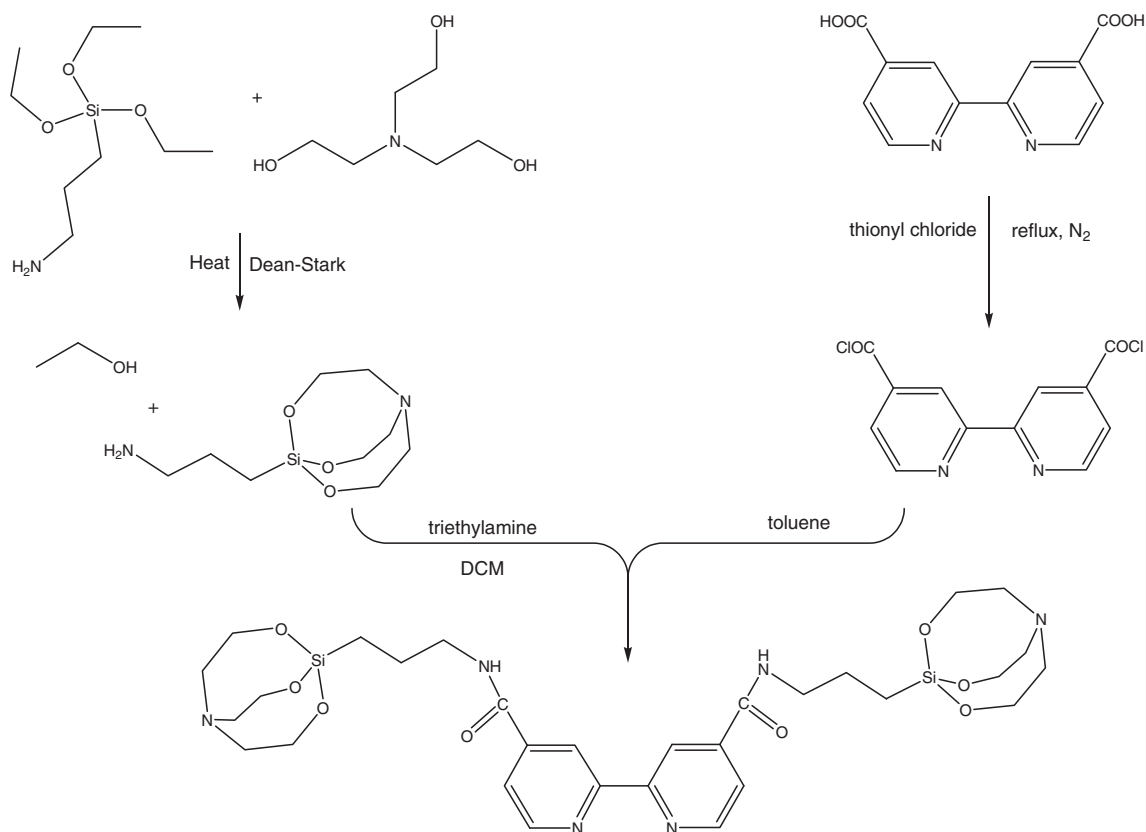
Scheme 2. Overall reaction sequence for the formation of tris-chelated Ru(II) complexes (1–3).

3.2. UV–Vis spectroscopy

UV–Vis absorption studies of tris-bipy complexes (Fig. 5): $[\text{Ru}(\text{bipy})_2(\text{dcbipy})](\text{PF}_6)_2$ (**1**), $[\text{Ru}(\text{bipy})_2(\text{dpbipy})](\text{PF}_6)_2$ (**2**), and $[\text{Ru}(\text{bipy})_2(\text{bipy-sil})](\text{PF}_6)_2$ (**3**) [29] were carried out in DMF solution at concentrations of 2, 3 and 4 mM. The molar extinction coefficients (Table 1) are averages of the three concentrations. In the

solid-state, all three complexes were orange-red in colour and this colour persisted in solution.

In the spectrum of $[\text{Ru}(\text{bipy})_2(\text{dcbipy})](\text{PF}_6)_2$ (**1**), one distinct band in the visible region between 400 and 600 nm was observed with a λ_{max} at 460 nm. The mean molar extinction coefficient of (**1**) was calculated to be $14350 \pm 320 \text{ L mol}^{-1} \text{ cm}^{-1}$ using the Beer–Lambert relationship (see Table 1 for a summary of λ_{max} and ϵ



Scheme 3. Reaction scheme for synthesis of *bipy-sil* [23].

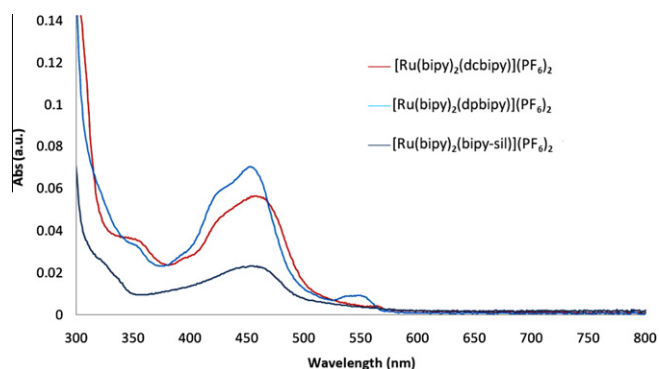


Fig. 5. UV-Vis spectra of complexes (1), (2) and (3) (3 mM, 300–800 nm).

data). The UV-Vis spectrum of the *dpibipy* complex $[\text{Ru}(\text{bipy})_2(\text{dpibipy})](\text{PF}_6)_2$ (2) is similar to that of the *dcbipy* complex (1), with a broad band observed between 400 and 500 nm ($\lambda_{\text{max}} = 450$ nm; shoulder $\lambda = 425$ nm), and a second small band at 545 nm. The structure of the absorption at 450 nm is characteristic of *tris-bipy* ruthenium complexes and arises from metal-to-ligand charge transfer (MLCT), from the metal t_2 orbital to the excited t_1 orbital [41,42]. The mean molar extinction coefficient of (2) was slightly higher than (1) at $17600 \pm 640 \text{ L mol}^{-1} \text{ cm}^{-1}$. The UV-Vis spectrum of the Brennan [23] *bipy-sil* complex, $[\text{Ru}(\text{bipy})_2(\text{bipy-sil})](\text{PF}_6)_2$ (3), is similar to both (1) and (2), with a λ_{max} at 457 nm, but with a lower absorbance. The mean molar extinction coefficient of (3) was calculated to be $10520 \pm 440 \text{ L mol}^{-1} \text{ cm}^{-1}$.

As stated previously, *tris-bipy* ruthenium complexes have limited absorbance in the visible region, which has been observed here in the UV-Vis spectra of complexes (1), (2) and (3). In all three

complexes, the bands are believed to arise from metal-to-ligand charge transfer (MLCT) transitions. The UV-Vis absorption studies of *bis-bipy* complexes, $[\text{Ru}(\text{dcbipy})_2\text{Cl}_2]$ (4), and $[\text{Ru}(\text{dcbipy})_2(\text{NCS})_2]$ (5), were carried out in acetonitrile solution. In the solid state, both (4) and (5) are dark red in colour, and this dark colour persisted in solution for complex (5), but (4) formed a red-pink solution. The UV-Vis spectrum of complex (4) exhibited one broad absorption band from 410 to 510 nm, with a pronounced shoulder from 420 to 440 nm, not unlike the absorbance profiles of (1) and (2). The absorption band of (4) had a λ_{max} at 467 nm, with a corresponding mean molar extinction coefficient of $20790 \pm 510 \text{ L mol}^{-1} \text{ cm}^{-1}$.

The UV-Vis spectrum of complex (5), the favoured commercial 'N3' dye, $[\text{Ru}(\text{dcbipy})_2(\text{NCS})_2]$, displayed two intense broad absorption bands in the visible region: band (1) from 425 to 550 nm ($\lambda_{\text{max}(1)} = 492$ nm, $\epsilon_{(1)} = 29630 \pm 870 \text{ L mol}^{-1} \text{ cm}^{-1}$); and band (2) from 610 to 750 nm ($\lambda_{\text{max}(2)} = 685$ nm, $\epsilon_{(2)} = 23380 \pm 690 \text{ L mol}^{-1} \text{ cm}^{-1}$) as seen in Fig. 6, which is characteristic of *bis-bipy* ruthenium complexes and has been reported previously for N3 [16].

UV-Vis absorption studies of the two new *bis-bipy-sil* complexes (6) and (7) were carried out in DMF solution. In the solid state both (6) and (7) are dark red in colour and this colour persisted in solution. Like the commercial N3 dye, two colour bands were observed in the spectrum of (6) $[\text{Ru}(\text{bipy-sil})_2\text{Cl}_2]$, one in the UV region, band (1) from 340 to 370 nm ($\lambda_{\text{max}(1)} = 365$ nm, $\epsilon_{(1)} = 12716 \pm 180 \text{ L mol}^{-1} \text{ cm}^{-1}$); and the second, band (2) in the visible from 440 to 540 nm ($\lambda_{\text{max}(2)} = 485$ nm, $\epsilon_{(2)} = 11070 \pm 150 \text{ L mol}^{-1} \text{ cm}^{-1}$).

The UV-Vis spectrum of complex, $[\text{Ru}(\text{bipy-sil})_2(\text{NCS})_2]$ (7) (Fig. 7), is similar to that observed in complex (6). But the bands in (7) are better defined and contain a band in the UV-region ranging from 340 to 400 nm (band (1) with λ_{max} at 371 nm and molar extinction coefficient of $20690 \pm 485 \text{ L mol}^{-1} \text{ cm}^{-1}$, and the second visible band range from 460 to 530 nm (band (2) with a λ_{max} at

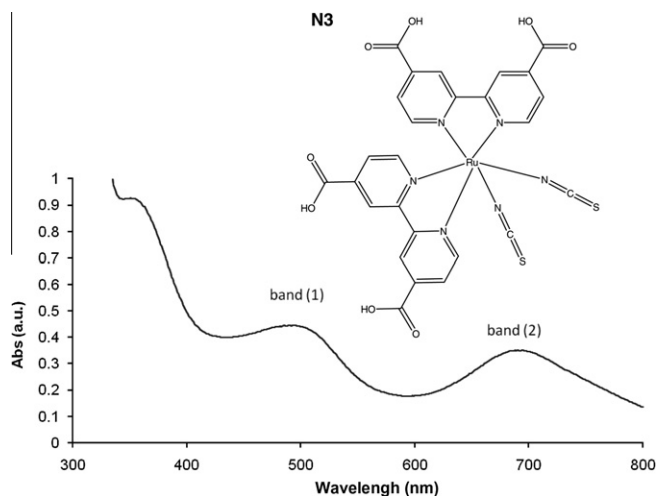


Fig. 6. UV-Vis spectrum of complex (5) 'N3 dye' (3 mM, 300–800 nm).

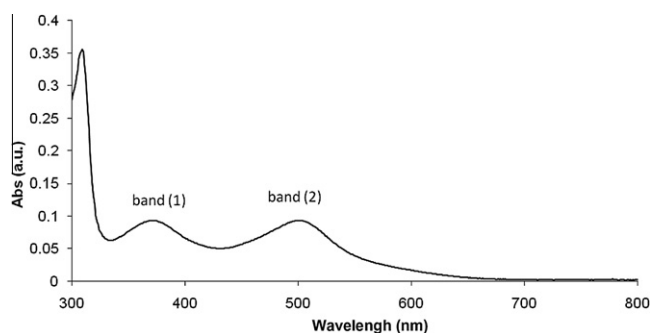


Fig. 7. UV-Vis spectrum of complex (7) (3 mM, 300–800 nm).

500 nm and molar extinction coefficient of $20750 \pm 487 \text{ L mol}^{-1} \text{ cm}^{-1}$. Hence, the absorbance and extinction coefficient values are significantly greater than those observed for (6), and the Brennan *bipy-sil* complex (3) [29].

As expected, the *bis-bipy* ruthenium complexes absorbed more visible light than the *tris-bipy* ruthenium complexes, as indicated by the presence of two absorption bands (Figs. 6 and 7) and the higher ϵ values (Table 1). The absorption bands have been assigned to metal-to-ligand charge transfer (MLCT) transitions, whilst the narrow intense bands at $\sim 300 \text{ nm}$ observed in the UV region are attributed to ligand $\pi-\pi^*$ transitions.

3.3. Solar cells

Clearly, the most efficient dye complexes will be those that: (a) absorb the most light; (b) are able to transfer the excited electron to the semi-conductor substrate; and (c) are readily reduced to the starting complex, to continue the photo-excitation redox cycle (see Fig. 1). All seven complexes (1)–(7) satisfy condition (a), which was

observed in their absorption data (refer to Table 1). But they require testing in a simulated solar cell to rate their efficiency in conditions (b) and (c). As mentioned earlier (Section 1), the surface binding of the carboxylic acid and phosphonic acid analogues is not stable across a wide pH range, however the silyl ester bond is, and this is one of its advantages [28]. The *tris-bipyridine* based ruthenium complexes were found to desorb from TiO_2 in aqueous solution at $\text{pH} \sim 4$ for the carboxylate, and $\text{pH} \sim 7$ for the phosphonate [24,28,29]. The stability of the silyl linkage allows it to function over a wider pH range and in the presence of significant amounts of organic solvents [43]. The silatrane is able to bind to the metal oxide surface after mild heating, upon which the triethanolamine group is lost and a silyl ester bond is formed at the surface, according to the reaction shown in Fig. 8.

All seven complexes were deposited successfully onto nano-structured TiO_2 and/or WO_3 films supported on an FTO-glass (Fluorine doped Tin Oxide) wafer. This was achieved by immersing an annealed, TiO_2 or WO_3 coated, FTO-glass substrate into a 0.3 mM solution of the dye species. Complexes (1) $[\text{Ru}(\text{bipy})_2(\text{dcbipy})](\text{PF}_6)_2$, (2) $[\text{Ru}(\text{bipy})_2(\text{dpbipy})](\text{PF}_6)_2$, (4) $[\text{Ru}(\text{dcbipy})_2\text{Cl}_2]$ and (5) $[\text{Ru}(\text{dcbipy})_2(\text{NCS})_2]$ were dissolved in acetonitrile or ethanol, and the substrate immersed in the solution for 24 h. Whilst complexes (3) $[\text{Ru}(\text{bipy})_2(\text{bipy-sil})](\text{PF}_6)_2$, (6) $[\text{Ru}(\text{bipy-sil})_2\text{Cl}_2]$ and (7) $[\text{Ru}(\text{bipy-sil})_2(\text{NCS})_2]$ were dissolved in DMF, and then heated gently at approximately 70°C for 1 h, under subdued light, in a glass container fitted with a condenser. The coated-substrates were then washed with ethanol, to remove excess dye, and air dried.

A thin film of the dye solution coated the substrate, as evidenced by a colour change. Attempts to quantify the degree of binding of the dye to the coated substrates by FT-IR or Raman spectroscopy were not successful, as there were no observable differences in the spectra of the pure semiconductor layer and that of the dye deposited on the semiconductor, despite an obvious change in the colour of the substrate. This is most likely due to the very thin film of the dye i.e. too low a concentration of the dye to be detected. As a result, the most effective way to determine whether the dye had adhered to the semiconductor was by visual comparison. Photographs of the DSSCs produced using complexes (1) to (7) are shown in Fig. 9.

The performance of the DSSCs was tested using a custom-made solar cell testing station, with a simulated solar light source. The recorded current and voltage for each of the solar cells is listed in Table 2. The voltage is the energy carried by the charge, and in DSSCs this corresponds to the difference between the Fermi level (which is the energy of the electrons in a semiconductor under illumination), compared to the Nernst potential of the electrolyte redox couple [4]. The macroscopic voltage and current are the sum total of all the individual molecular photo-excitation events. It is found that the array generates a voltage which can be modelled as a series of cells linked in parallel. Hence, the numerical value of the voltage is determined by the characteristics of the dye/semiconductor combination, and its capacity (total Joule/Coulomb) by the number of such molecular units in the array [4,44–46].

The current is directly linked to the efficiency of electron transfer between the semiconductor and the dye, and the reductive

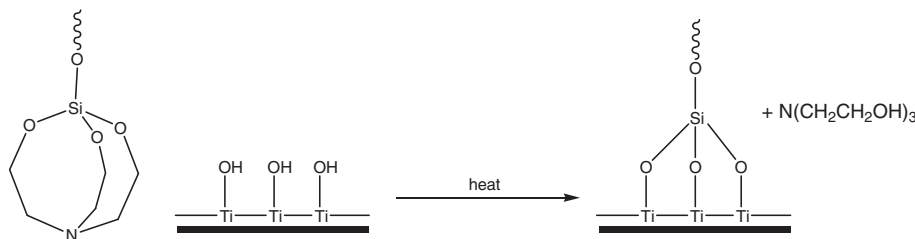


Fig. 8. Silyl linkage: "chemisorption" to TiO_2 .

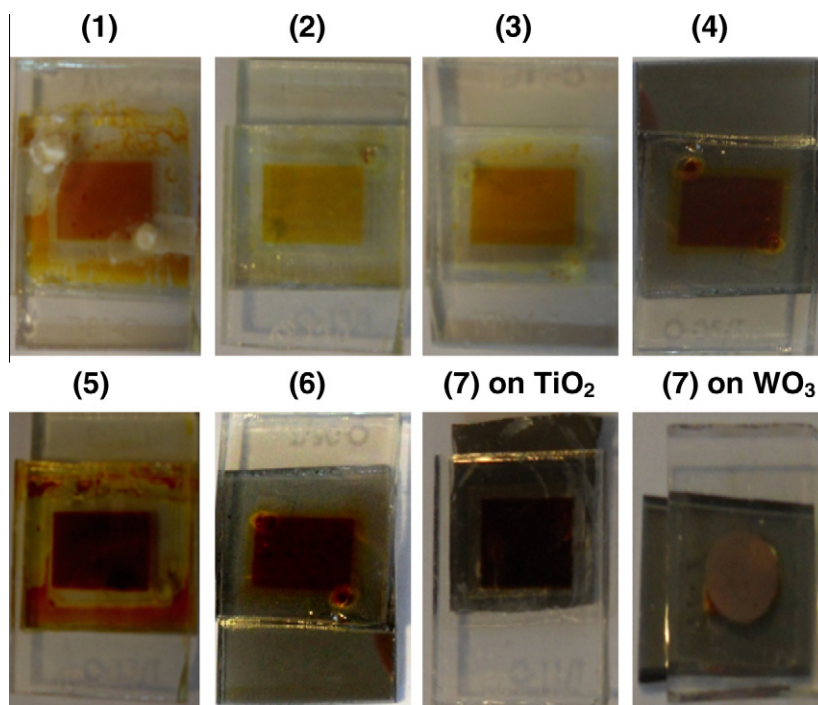


Fig. 9. Photos of DSSCs produced using complexes (1)–(7).

Table 2

Current, voltage and efficiency of DSSCs prepared on TiO₂/FTO (1)–(7), and WO₃/FTO (7).

Dye	Number	Short circuit current density, I_{sc} (mA)	Open circuit voltage, V_{oc} (mV)	Fill factor (ff) ^a	Efficiency (%) ^b
[Ru(<i>bipy</i>) ₂ (<i>dcbipy</i>)](PF ₆) ₂	(1)	0.184	390	0.19	0.015
[Ru(<i>bipy</i>) ₂ (<i>dpbipy</i>)](PF ₆) ₂	(2)	0.002	140	0.24	0.00007
[Ru(<i>bipy</i>) ₂ (<i>bipy-sil</i>)](PF ₆) ₂	(3)	0.110	160	0.23	0.0045
[Ru(<i>dcbipy</i>) ₂ Cl ₂]	(4)	1.000	590	0.25	0.164
[Ru(<i>dcbipy</i>) ₂ (NCS) ₂] N3	(5)	1.352	650	0.26	0.254
[Ru(<i>bipy-sil</i>) ₂ Cl ₂]	(6)	0.163	350	0.25	0.016
[Ru(<i>bipy-sil</i>) ₂ (NCS) ₂]	(7) TiO ₂	0.360	480	0.27	0.052
[Ru(<i>bipy-sil</i>) ₂ (NCS) ₂]	(7) WO ₃	0.985	160	0.23	0.040

^a The fill factor (ff) was calculated using Eq. (2) [2]

$$ff = \frac{I_{mpp} \times V_{mpp}}{I_{sc} \times V_{oc}} \quad (2)$$

I_{mpp} is the current measured at the power point (maximum), the power point is the maximum product obtained from the cell voltage and current. V_{mpp} is the voltage measured at the power point (maximum). I_{sc} is the photocurrent density. V_{oc} is the voltage measured at short circuit.

^b The efficiency was calculated using the 'power conversion efficiency' Eq. (3) [2]

$$\eta_{global} = \frac{I_{sc} V_{oc} ff}{I_s} \quad (3)$$

η_{global} is the Overall conversion efficiency. ff is the "fill factor", which is the ratio of the maximum power output of the cell to the potential power output of the cell. I_s is the intensity of the incident light (90 mW/cm² from calibration).

regeneration of the metal centre. The current can be modelled as a series sum of the number of electrons collected from each molecular event; it is this factor which is critical in the efficiency of photon-to-electrical conversion, and will be dependent on the extent of coating, the tightness of dye binding, and the facilitation of e^- transfer from the dye to the semiconductor [4,13,44–46].

The *tris-bipy* complexes (1) to (3) formed light yellow-orange layers on the semiconducting surface, the light colour of the dye on the surface implies that only a limited amount of dye has been adsorbed on the oxide (two anchoring groups compared to four in the *bis-bipy* derivatives). This in turn limits the amount of light which can be absorbed, and therefore a high current or voltage

was not expected. The main purpose of investigating the *tris-bipy* ruthenium complexes was to compare them with the *bis-bipy* complexes and note any effects of the anchoring ligands. In particular, the Brennan complex [29], which is the only previous report of a *tris-bipy-sil* complex binding to a semiconductor substrate (in their case SnO₂). To the best of our knowledge, dye complexes containing silyl linkers have not been tested previously in TiO₂ or WO₃ based DSSCs.

Of this group, the anchoring ligand which gave the best current, voltage and overall efficiency was *dcbipy* (1) whilst *dpbipy* (2) gave surprisingly low results considering that the molar extinction coefficient of complex (2), [Ru(*bipy*)(*dpbipy*)](PF₆)₂, was the highest of

the three *tris-bipy* complexes ($17603 \text{ L mol}^{-1} \text{ cm}^{-1}$), indicating strong light absorption in solution. The *bipy-sil* complex (**3**) [29] gave about 60% of the current, and 40% of the voltage observed for the *dcbipy* complex (**1**). The efficiency of this cell is therefore quite low; approximately 30% that of the *dcbipy* complex cell. This is likely due to inefficient electron-transfer through the long saturated propyl chain of the silyl linker.

Considerably more promising results were attained for the *bis-bipy* systems. Complex (**4**), $[\text{Ru}(\text{dcbipy})_2\text{Cl}_2]$, formed a dark orange-red layer on the semiconductor surface, and the voltage (590 mV) and current (1 mA) of the cell were good. These results improved for the commercially-favoured dithiocyanato analogue, (**5,N3**) $[\text{Ru}(\text{dcbipy})_2(\text{NCS})_2]$, which gave a dark orange-red layer on the semiconductor surface, and a measured current and voltage of 1.352 mA and 650 mV, respectively. Complex (**6**), $[\text{Ru}(\text{bipy-sil})_2\text{Cl}_2]$, formed a dark red layer on the semiconductor surface, but despite the appearance, the current (0.163 mA) and voltage (350 mV) were quite low, with the measured fill-factor of 25%, then the overall efficiency of the dye is 0.016%. This is however, on comparison with (**3**) [29], a 4-fold increase in efficiency.

Complex (**7**), $[\text{Ru}(\text{bipy-sil})_2(\text{NCS})_2]$, gave a significant improvement in the current, voltage and overall efficiency when compared to (**6**) and (**3**). Complex (**7**) also formed a dark-red film over the TiO_2 . Whilst (**6**) and (**3**) contain the same silyl ligand, complex (**7**) also contains the thiocyanate anion which is known to improve efficiency and extend wavelength absorption (see Fig. 7). The measured current and voltage were 0.360 mA and 480 mV, respectively, and the overall efficiency 0.052%. Thus, for (**7**), the voltage has increased by 130 mV, and the current, and hence the overall efficiency, has increased 4-fold compared to that of (**6**), and increased 10-fold to that of (**3**) [29]. Therefore, by changing the counter-anion from Cl^- to NCS^- the efficiency of the *bipy-sil* based cell can be improved considerably.

Amongst the solar energy community, there is also interest in using the intrinsic semiconductor, WO_3 , as a substrate in DSSCs, as WO_3 can absorb light directly. When complex (**7**) was adsorbed onto a WO_3 semiconductor substrate, the current measured (0.985 mA) was significantly higher than that observed with the same complex adsorbed on TiO_2 (0.360 mA), and comparable to that of the *bis-dcbipy* complex (**4**). However, the voltage measurement was significantly lower at 160 mV and is attributed to a combination of low dye coverage, which may be due to poor adhesion of the dye to the substrate, and the difference between the Fermi level of WO_3 , when compared to the Nernst potential.

In summary, the measured current and voltage, on TiO_2 substrates, of the two new *bis-bipy-sil* complexes (**6**) and (**7**) which contain silyl linkages, are lower than those of *bis-dcbipy* analogues (**4**) and (**5**), but significant improvements to the overall efficiency have been achieved by replacing the chloride counter ion with thiocyanate, and there is considerable potential for further improvement through modification of the silyl linker.

3.4. Synthesis of modified silyl linkers

The presence of saturated bonds in the bridge between the anchoring group and the dye is known to lower the efficiency of electronic coupling between the dye and the semiconductor substrate [47]. Thus, the non-conjugated propyl chain between the amide group and the silatrane (*bipy-sil*) in (**6**) and (**7**) is likely to reduce electron transfer significantly (Fig. 10). To improve this transfer/efficiency, the linker either needs to incorporate conjugation, e.g. replace the propyl chain with a phenyl group, or the distance between the dye and substrate needs to be considerably shorter e.g. by removal of the amide-propyl group (Fig. 10). The former strategy was considered, but the cost of the starting material proved prohibitive, and thus not a viable option. More

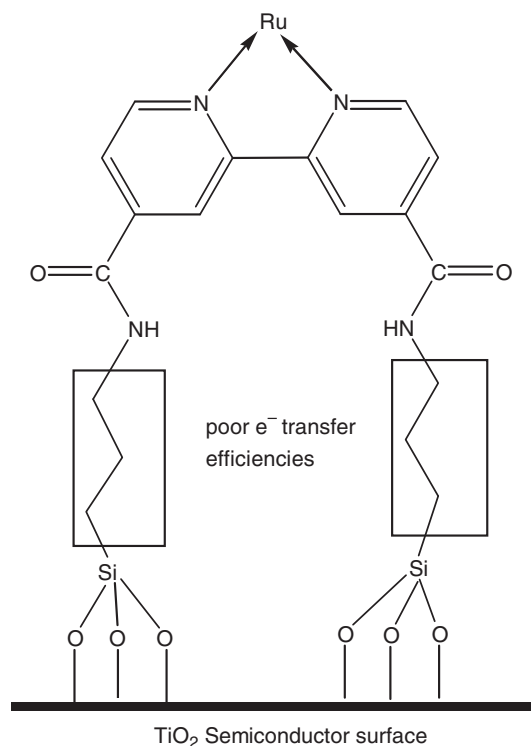


Fig. 10. The long, non-conjugated propyl chain linker of *bipy-sil* to TiO_2 .

favourable strategies were: (a) *direct addition* (Si–C) of a silatrane group to the bipyridine ligand, (b) *amide linkage* (Si–N(H)–C(O)–C), or (c) *ester linkage* (using a carboxylate group – Si–O–C(O)–C), as indicated in Fig. 11.

Strategy (a) *direct linkage* was investigated initially, in an attempt to produce the target ligand: *4,4'-disilatrane-2,2'-bipyridine*. Three different organic schemes ((1) Grignard reagent, (2) Pd-catalyst, and (3) butyllithium), using a silatrane form of tetraethylorthosilicate (TEOS) (in place of 1-(3-aminopropyl)triethoxysilane used in *bipy-sil* synthesis) were trialled.

3.4.1. (a) Direct linkage: (1) Grignard reagent method

The predicted reaction sequence, using 4,4'-dibromo-2,2'-bipyridine (*bipy-Br₂*) as the starting material, is illustrated in Fig. 12. Two methods were investigated to activate the magnesium turnings, dibromoethane and iodide. Dibromoethane was found to be an ineffective activating agent for the bipyridine. This result

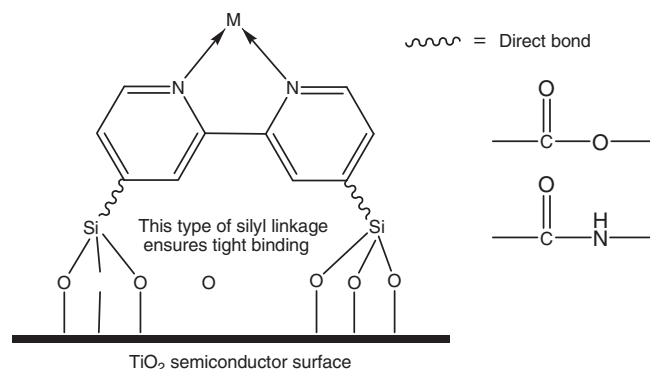


Fig. 11. Short silyl linkage options: direct addition (Si–C); amide linkage (Si–N(H)–C(O)–C); and ester linkage (Si–O–C(O)–C).

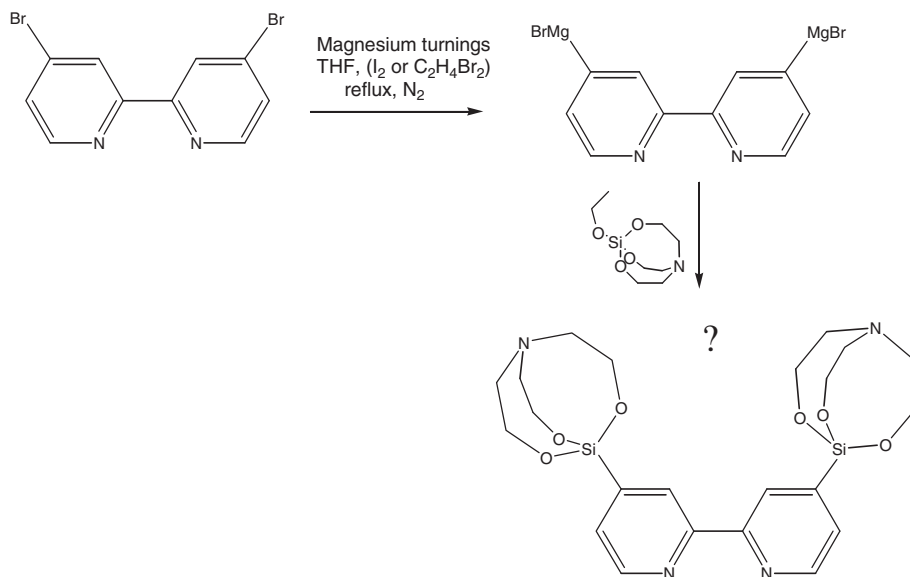


Fig. 12. Grignard reaction sequence – target ligand 4,4'-disilatrane-2,2'-bipyridine.

was not unexpected as a similar method, whereby 2-bromopyridine was reacted with magnesium powder and dibromoethane under sonication, has been reported in the literature [48], and was also found to be unsuccessful. Iodine, a more aggressive activator, appeared to be more effective in activating the magnesium – oxidation was observed at the magnesium surface. However, reaction of the subsequent 'Grignard reagent' with 1-ethoxysilatrane was ultimately unsuccessful, and NMR and mass spectroscopy confirmed that only the starting materials *bipy-Br*₂ and 1-ethoxysilatrane, were isolated.

It is possible that the Grignard reagent did not form: this is difficult to ascertain, as isolation of the reagent is often not possible owing to its instability, and thus immediate use is preferential. Also, whilst Grignard reagents are able to form quite readily with phenyl rings, pyridine rings generally prove to be more troublesome. Nitrogen is more electronegative than carbon, and therefore the carbon π -orbitals may be more attracted to the nitrogen atom thus deforming the orbitals, and consequently producing π -deficient pyridine rings [49]. In addition to this, the lone pair of electrons on the nitrogen are basic and not delocalised over the ring. Subsequently, a Pd-catalysed reaction was investigated as an alternative.

3.4.2. (a) Direct linkage: (2) Pd-catalysed method

The second route employed a Palladium-catalyst, Pd(PPh₃)₄. The use of Pd-catalysts in organic synthesis has been studied extensively, in particular for the formation of C–C bonds. Indeed, in this paper, and in the literature [37], a Pd-catalyst was used successfully to form a C–P bond, in the synthesis of 4,4'-diphosphonic acid-2,2'-bipyridine (*dpbipy*). However, the use of a Pd-catalyst with *bipy* may lead to deactivation of the Pd-catalyst, as *bipy* can compete with the triphenylphosphine ligand for coordination to the metal centre. To limit this from occurring, a large excess of triphenylphosphine was added to the reaction mixture [50–51]. The initial oxidative-addition of the Pd-catalyst is analogous to the formation of the Grignard reagent, where the carbon–halogen covalent bond is cleaved to form a new complex. However, this method was also unsuccessful. NMR data indicating that only the bipyridine starting material was isolated.

3.4.3. (a) Direct linkage: (3) Butyllithium method

The third synthetic method for direct linkage involved the use of butyllithium, which out of all the methods attempted in forming a direct silicon–carbon bond, was the most successful. Riedmiller et al. have reported the successful reaction of *n*-butyllithium and TEOS at –78 °C under N₂ to form 3-triethoxysilylpyridine [32]. In general, this method has been found to be successful for the formation of *ortho*- and *meta*-substituted bromo-pyridine systems, but *para*-substituted bromo-pyridine systems were not investigated. The Riedmiller et al. [32] method was adapted here using 4,4'-dibromo-2,2'-bipyridine and 1-ethoxysilatrane instead of 3-bromopyridine and tetraethoxysilane. NMR data of the product indicated that peaks corresponding to the silatrane group and aromatic groups were present, although not in the expected ratios. Unfortunately, the product decomposed rapidly, and hence further analysis could not be undertaken. This route was therefore not considered to be viable, as the compound was unstable under ambient conditions.

In summary, the formation of a direct Si–C bond from a Br–C bond in a *para*-substituted bromopyridine ring was not found to be possible by any of the three organic routes, using 1-ethoxysilatrane. This may be due to the pyridyl-nitrogen atoms inhibiting the formation of a direct bond, the insufficient reactivity of the 1-ethoxysilatrane group to enable this formation, and/or the bulky nature of the latter. Attempts to react *bipy-Br*₂ with 1-chlorosilatrane were also unsuccessful. In a final attempt to form a direct Si–C bond on *bipy*, a more reactive and less-bulky group (trimethylsilyl, TMS) was investigated. 4,4'-di(trimethylsilyl)-2,2'-bipyridine was produced successfully by reaction of TMS-Cl with 4,4'-dibromo-2,2'-bipyridine, as confirmed by ¹H NMR data (see Section 2). Unfortunately, the material proved to be extremely unstable, decomposing rapidly in the presence of air, and could not be tested in a DSSC.

3.4.4. (b) Amide linkage: (1) TMS-Cl and 1-chlorosilatrane method

To determine whether a silicon–amide bond (Si–NH–C(O)), or a direct silicon bond (Si–C) to the pyridine ring would be possible, reaction of trimethylsilyl chloride (TMS-Cl) with an amide-pyridine or bromo-pyridine, followed by reaction with 1-chlorosilatrane (a more reactive group than ethoxy), was investigated. *N*-(trimethylsilyl)pyridine-3-carboxamide has been prepared

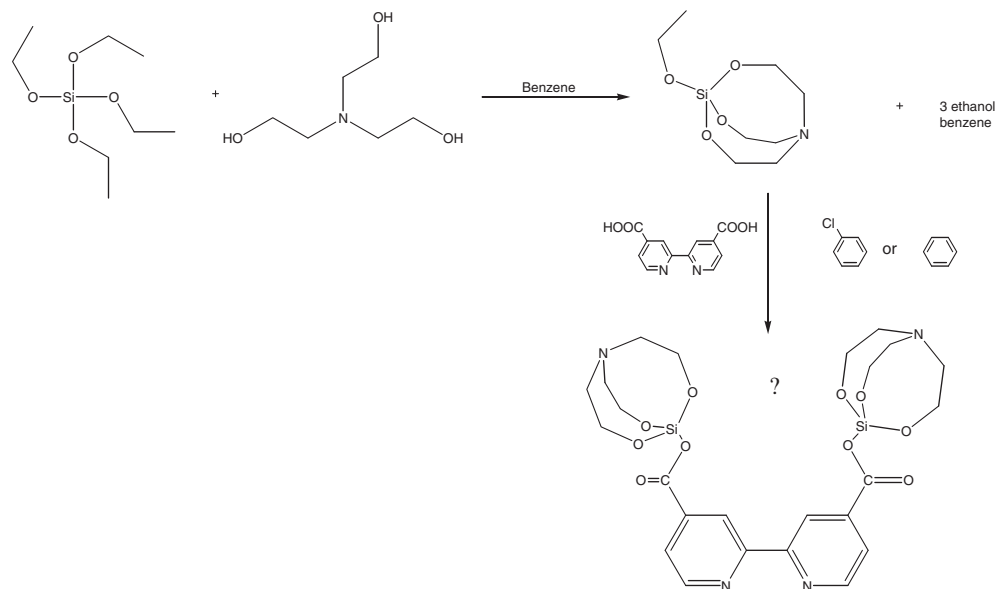


Fig. 13. Carboxy-sil reaction sequence – target ligand 4,4'-dicarboxysilatrane-2,2'-bipyridine.[46].

previously by Gilg et al. [34,35], and this was repeated successfully in this work (as confirmed by ^1H NMR data, see Section 2). However, reaction of nicotinamide with 1-chlorosilatrane (target ligand; *N*-(1-silatranyl)nicotinamide) proved to be more difficult, with no reaction taking place. This route was therefore not explored with substituted *bipy* derivatives. As with the Grignard (direct Si–C) route, a possible reason for the lack of reaction may be due to the bulkier nature of the silatrane group when compared to that of trimethylsilyl. There is also the possibility that the hexamethyldisilazane may compete with the chlorosilatrane for bonding to the ring, and it may be possible that both hexamethyldisilazane and TMS–Cl contribute to the formation of an amide-silicon bond. Synthetic methods in which hexamethyldisilazane was replaced by e.g. benzene, toluene, chlorobenzene were also investigated, but unfortunately, were also unsuccessful.

3.4.5. (c) Ester linkage: (i) Carboxy-sil method

As strategies (a) – direct linkage, and (b) – amide linkage, were unsuccessful, the formation of a carboxy-sil bond (Si–O–C(O)) was considered. This type of bonding has been observed previously with ferrocenyl carboxylic acid and 1-ethoxysilatrane [52], where, a carboxylic acid and a silatrane were reacted together in an azeotropic solvent to form 1-ferrocenecarboxysilatrane. This method was successful for Chen et al. [52], with isolation of 1-ferrocenecarboxysilatrane in good yields and crystals of suitable quality for single-crystal XRD analysis. Ferrocene is able to undergo similar reactions to those observed with aromatic compounds.

Owing to the success of Chen et al. [52] a similar method, using the reaction scheme illustrated in Fig. 13, was explored. However, as observed with the other routes, a mixture of starting materials was isolated. The NMR spectrum indicated the presence of aromatic and methylene protons, however mass spectroscopy suggested that no new oxygen-silicon bond had formed. This result is not surprising, as this bond is known to be quite unstable, decomposing rapidly [43]. This point is further emphasised by the limited amount of research in this field [53].

4. Conclusion

The efficiency, and efficacy of a new silyl linker, *bipy-sil*, for binding ruthenium(II) bipyridine chromophores to metal oxides

in DSSCs, was tested and compared to previously favoured carboxylate (*dcbipy*) and phosphonate (*dpbipy*) anchors. The *bipy-sil* linker has been trialled on SnO_2 [29], but has not been explored previously with TiO_2 or WO_3 DSSC systems.

The linkers were examined as both *tris-bipy* systems: $[\text{Ru}(\text{bipy})_2(\text{dcbipy})](\text{PF}_6)_2$ (**1**), $[\text{Ru}(\text{bipy})_2(\text{dpbipy})](\text{PF}_6)_2$ (**2**), and (**3**) $[\text{Ru}(\text{bipy})_2(\text{bipy-sil})](\text{PF}_6)_2$, and *bis-bipy* systems with either *cis*-dichloro: $[\text{Ru}(\text{dcbipy})_2\text{Cl}_2]$ (**4**) and $[\text{Ru}(\text{bipy-sil})_2\text{Cl}_2]$ (**6**), or *cis*-dithiocyanato ligands: $[\text{Ru}(\text{dcbipy})_2(\text{NCS})_2]$ (**5**) and $[\text{Ru}(\text{bipy-sil})_2(\text{NCS})_2]$ (**7**). From UV–Vis spectroscopy solution measurements, all seven complexes were found to have the desired properties for solar energy capture. Whilst the commercial carboxylate linker, *dcbipy*, was found to outperform the phosphonate linker, *dpbipy*, and the silyl linker, for both the *tris-bipy* and *bis-bipy* systems, in terms of the current, voltage and efficiency of their respective DSSC cells, it must be said that this is the first test of a silyl linker in TiO_2 and WO_3 DSSCs, and that the overall performance of the silyl linker in TiO_2 based cells has been significantly improved over the course of this study. A 10-fold increase in efficiency was attained in moving from the Brennan complex, $[\text{Ru}(\text{bipy})_2(\text{bipy-sil})](\text{PF}_6)_2$ (**3**) [29], to $[\text{Ru}(\text{bipy-sil})_2\text{Cl}_2]$ (**6**) to $[\text{Ru}(\text{bipy-sil})_2(\text{NCS})_2]$ (**7**). Also, despite the disappointing voltage of (**7**) on WO_3 , the current was comparable to that of the *dcbipy*- TiO_2 system (**4**), $[\text{Ru}(\text{dcbipy})_2\text{Cl}_2]$. Further experiments to optimise the binding of (**7**) to WO_3 are likely to extend the performance well beyond that of the currently-favoured **N3** dye (**5**), $[\text{Ru}(\text{dcbipy})_2(\text{NCS})_2]$, on TiO_2 .

In this work, despite significant effort, strategies to synthesise 4,4'-disilyl-functionalised bipyridyl ligands, with a short distance (more efficient e-transfer pathway) between the Si link and the *bipy* framework, by formation of (a) direct Si–C bonds, (b) amide Si–NH–C(O) links, or (c) ester Si–O–C(O) bonds to the silatrane, proved unsuccessful, or the products were insufficiently stable to allow their incorporation into Ru(II) complexes, and subsequent DSSC fabrication. It is however, believed that the silyl linkage will be an important component of more robust dyes used to sensitise metal oxide surfaces (TiO_2 , WO_3 , ZnO , SnO_2 , etc.) and it is therefore recommended that further studies be pursued in this challenging synthetic area. The most promising strategy in this work appears to be direct linkage (a), the formation of a direct Si–C bond, using butyllithium with 4,4'-dibromo-2,2'-bipyridine and either trimethylsilane or 1-ethoxysilatrane, provided that the product can be

captured and stabilised prior to binding to a metal oxide coated DSSC substrate. This may have to be done in an enclosed, dry environment, possibly *in-situ*.

Appendix A. Supplementary data

Supplementary data associated with this article can be found, in the online version, at <http://dx.doi.org/10.1016/j.poly.2012.07.078>.

References

- [1] T.W. Hamann, R.A. Jensen, A.B.F. Martinson, H. Van Ryswyk, J.T. Hupp, *Energy Environ. Sci.* 1 (1) (2008) 66.
- [2] Z. Ning, Y. Fu, H. Tian, *Energy Environ. Sci.* 3 (9) (2010) 1170.
- [3] S. Campagna, F. Puntoriero, F. Natasi, G. Bergamini, V. Balzani, *Top. Curr. Chem.* 280 (117) (2007) 214.
- [4] M.K. Nazeeruddin, M. Grätzel, in: J.A. McCleverty, T.J. Meyer (Eds.), *Comprehensive Coordination Chemistry II*, vol. 9, Elsevier, Pergamon, 2004.
- [5] S. Chappel, S.G. Chen, A. Zaban, *Langmuir* 18 (8) (2002) 3336.
- [6] Q. Zhang, C.S. Dandeneau, X. Zhou, G. Cao, *Adv. Mater.* 21 (41) (2009) 4087.
- [7] H. Zheng, Y. Tachibana, K. Kalantar-zadeh, *Langmuir* 26 (2010) 19148.
- [8] J.Z. Ou, R.A. Rani, M.-H. Ham, M.R. Field, Y. Zhang, H. Zheng, P. Reece, S. Zhuiykov, S. Sriram, M. Bhaskaran, R.B. Kaner, K. Kalantar-zadeh, *ACS NANO* 6 (5) (2012) 4045.
- [9] N. Alonso-Vante, J.-F. Nierengarten, J.-P. Sauvage, *J. Chem. Soc., Dalton Trans.* (1994) 1649.
- [10] E. Bae, W. Choi, *J. Phys. Chem. B* 110 (2006) 14792.
- [11] M. Grätzel, *Prog. Photovolt. Res. Appl.* 8 (2000) 171.
- [12] M. Grätzel, *Nature* 414 (2001) 338.
- [13] M. Grätzel, *J. Photochem. A* 164 (2004) 3.
- [14] A. Hagfeldt, M. Grätzel, *Chem. Rev.* 95 (1995) 49.
- [15] M.K. Nazeeruddin, P. Pechy, M. Grätzel, *Chem. Commun.* (1997) 1705.
- [16] M.K. Nazeeruddin, S.M. Zakeeruddin, R. Humphry-Baker, M. Jirousek, P. Liska, N. Vlachopoulos, V. Shklover, C.-H. Fischer, M. Grätzel, *Inorg. Chem.* 38 (1999) 6298.
- [17] K. Kalyanasundaram, M. Grätzel, *Coord. Chem. Rev.* 77 (1998) 347.
- [18] M. Grätzel, *J. Photochem. Photobiol. C* 4 (2003) 145.
- [19] R. Argazzi, C.A. Bignozzi, T.A. Heimer, F.N. Castellano, G.J. Meyer, *Inorg. Chem.* 33 (1994) 5741.
- [20] P. Wang, C. Klein, J.-E. Moser, R. Humphry-Baker, N.-L. Cevey-Ha, R. Charvet, P. Comte, S.M. Zakeeruddin, M. Grätzel, *J. Phys. Chem. B* 108 (2004) 17553.
- [21] P. Liska, N. Vlachopoulos, M.K. Nazeeruddin, P. Comte, M. Grätzel, *J. Am. Chem. Soc.* 110 (1988) 3686.
- [22] M.K. Nazeeruddin, P. Pechy, T. Renouard, S.M. Zakeeruddin, R. Humphry-Baker, P. Comte, P. Liska, L. Cevey, E. Costa, V. Shklover, L. Spiccia, G.B. Deacon, C.A. Bignozzi, M. Grätzel, *J. Am. Chem. Soc.* 123 (2001) 1613.
- [23] M.K. Nazeeruddin, A. Kay, I. Rodicio, R. Humphry-Baker, E. Müller, P. Liska, N. Vlachopoulos, M. Grätzel, *J. Am. Chem. Soc.* 115 (1993) 6382.
- [24] E. Bae, W. Choi, J. Park, H.S. Shin, S.B. Kim, J.S. Lee, *J. Phys. Chem. B* 108 (2004) 14093.
- [25] P.A. Anderson, G.F. Strouse, J.A. Treadway, F.R. Keene, T.J. Meyer, *Inorg. Chem.* 33 (1994) 3863.
- [26] V.M. Cristante, A.G.S. Prado, S.M.A. Jorge, J.P.S. Valente, A.O. Florentino, P.M. Padilha, *J. Photochem. Photobiol. A* 195 (2008) 23.
- [27] P.K. Ghosh, T.G. Spiro, *J. Am. Chem. Soc.* 102 (1980) 5543.
- [28] A.K.M. Fung, B.K.W. Chiu, M.H.W. Lam, *Water Res.* 37 (2003) 1939.
- [29] B.J. Brennan, A.E. Keirstead, P.A. Liddell, S.A. Vail, T.A. Moore, A.L. Moore, *Nanotechnology* 20 (2009) 505203.
- [30] V.V. Semenov, N.F. Cherepennikova, S.Y. Khorshev, T.G. Mushtina, M.A. Lopatin, G.A. Domrachev, *Russ. J. Coord. Chem.* 28 (2002) 856.
- [31] V.V. Kazakova, O.B. Gorbatshevich, S.A. Skvortsova, N.V. Demchenko, A.M. Muzafarov, *Russ. Chem. Bull. Int. Ed.* 54 (2005) 1350.
- [32] F. Reidmiller, A. Jockisch, H. Schmidbaur, *Organometallics* 17 (1998) 4444.
- [33] D.G. Anderson, M.A.M. Bradney, D.E. Webster, *J. Chem. Soc. B* (1968) 450.
- [34] K. Gilg, P. Klüfers, *Acta Crystallogr., Sect. E* 63 (2007) 4764.
- [35] P. Franchetti, M. Pasqualini, R. Petrelli, M. Ricciutelli, P. Vita, L. Cappellacci, *Bioorg. Med. Chem. Lett.* 14 (2004) 4655.
- [36] L. Chen, Q. Xie, L. Sun, H. Wang, *J. Org. Chem.* 678 (2003) 90.
- [37] K. Kanaizuka, S. Kato, H. Moriyama, C. Pac, *Res. Chem. Intermed.* 33 (2007) 91.
- [38] G. Sprintschnik, H.W. Sprintschnik, P.P. Kirsch, D.G. Whitten, *J. Am. Chem. Soc.* 99 (1977) 4947.
- [39] W.R. Browne, P. Passaniti, M.T. Gandolfi, R. Ballardini, W. Henry, A. Guckian, N. O'Boyle, J.J. McGarvey, J.G. Vos, *Inorg. Chim. Acta* 360 (2007) 1183.
- [40] E. Terpetschnig, H. Szmecinski, H. Malak, J.R. Lakowicz, *Biophys. J.* 68 (1995) 342.
- [41] K. Kalyanasundaram, *Coord. Chem. Rev.* 46 (1982) 159.
- [42] A. Juris, V. Balzani, F. Barigelli, S. Campagna, P. Belsler, A.v. Zelewsky, *Coord. Chem. Rev.* 84 (1988) 85.
- [43] H. Hügel, personal communication, 2011.
- [44] F.-T. Kong, S.-Y. Dai, K.-J. Wang, *Adv. Optoelectron.* 75384 (2007) 1.
- [45] F.O. Lenzmann, J.M. Kroon, *Adv. Optoelectron.* 65073 (2007) 1.
- [46] Q. Wang, S. Ito, M. Grätzel, F. Fabregat-Santiago, I. Mora-Ser, J. Bisquert, T. Bessho, H. Imai, *J. Phys. Chem. B* 110 (2006) 25210.
- [47] E. Galoppini, *Coord. Chem. Rev.* 248 (2004) 1283.
- [48] A.S.-Y. Lee, Y.-T. Chang, S.-F. Chu, K.-W. Tsao, *Tetrahedron Lett.* 47 (2006) 7085.
- [49] P. Sykes, *A Guide to Mechanisms in Organic Chemistry*, sixth ed., Longman Scientific & Technical, Singapore, 1986.
- [50] V. Penicaud, F. Odobel, B. Bujoli, *Tetrahedron Lett.* 39 (1998) 3689.
- [51] A.S. Manoso, P. DeShong, *J. Org. Chem.* 66 (2001) 7449.
- [52] L. Chen, Q. Xie, L. Sun, H. Wang, *J. Organomet. Chem.* 678 (2003) 90.
- [53] M.G. Voronkov, G. Zelcans, Institute of Organic Synthesis, Academy of Sciences, Latvian SSR, USSR, 1968.